

Density-valued time series: Nonparametric density-on-density regression

Frédéric Ferraty 

Toulouse Mathematics Institute
University of Toulouse

Han Lin Shang  *

Department of Actuarial Studies and Business Analytics
Macquarie University

Abstract

This paper is concerned with forecasting probability density functions. Density functions are nonnegative and have a constrained integral; they thus do not constitute a vector space. Implementing unconstrained functional time-series forecasting methods is problematic for such nonlinear and constrained data. A novel forecasting method is developed based on a nonparametric function-on-function regression, where both the response and the predictor are probability density functions. Through a series of Monte-Carlo simulation studies, we evaluate the finite-sample performance of our nonparametric regression estimator. Using French departmental COVID19 data and age-specific period life tables in the United States, we assess and compare finite-sample forecast accuracy between the proposed and several existing methods.

Keywords: Bayes space; Convex constraint; Density forecasting; Nonparametric function-on-function regression; Time series of densities.

Short Run Title: Nonparametric density-on-density regression

1 Introduction

Recent advances in computer storage and data collection have enabled researchers to record data of characteristics varying over a continuum (time, space, depth, wavelength, etc.). In diverse branches of science, the data are collected by a spectrometer, rain gauges, electroencephalographs, or even a high-performance computer. In all these cases, a number of subjects are observed densely over time, space, or both. Through the application of interpolation or smoothing techniques,

*Postal address: Department of Actuarial Studies and Business Analytics, Level 7, 4 Eastern Road, Macquarie University, Sydney NSW 2109, Australia; Telephone: +61(2) 9850 4689; Email: hanlin.shang@mq.edu.au

these data become functions that can be represented as a curve, image, or shape. Functional data analysis has arisen as a field of statistics that provides statistical tools for analyzing this type of information. For an overview of functional data analysis, [Ramsay & Silverman \(2005\)](#) presented several state-of-the-art statistical techniques while [Ferraty & Vieu \(2006\)](#) listed a range of nonparametric techniques. [Hsing & Eubank \(2015\)](#) provided theoretical foundations with an introduction to linear operators, while [Bosq \(2000\)](#) studied functional autoregressive process from a linear operator perspective. An introduction to temporally dependent functional data can be found in [Kokoszka & Reimherr \(2017\)](#), while [Mateu & Giraldo \(2022\)](#) studied spatially-dependent functional data.

As an integral part of functional data analysis and time series analysis, functional time series consist of random functions observed at a time interval. Functional time series can be classified into two categories depending on whether the continuum is also a time variable. On the one hand, when the continuum is not a time variable, functional time series can also arise when observations in a period can be considered as finite-dimensional realisations of an underlying continuous function. Examples include yearly age-specific mortality rates (see, e.g., [Chiou & Müller 2009](#), [Hyndman & Shang 2009](#)) and a time series of near-infrared spectroscopy curves (see, e.g., [Shang et al. 2022](#)). On the other hand, functional time series can arise from measurements obtained by separating a continuous-time stochastic process into natural consecutive intervals, for example, days, weeks, or years (see, e.g., [Bosq 2000](#), [Besse et al. 2000](#), [Antoniadis & Sapatinas 2003](#), [Antoniadis et al. 2006](#), [Ferraty & Vieu 2006](#), [Hörmann & Kokoszka 2012](#), [Kokoszka et al. 2017](#), [Shang 2017](#)).

Functional data that are samples of one-dimensional random probability density functions (PDFs) are common. Examples include income distributions ([Kneip & Utikal 2001](#)), distributions of the times when bids are submitted in an online auction ([Jank et al. 2008](#)), functional connectivity in the brain ([Petersen & Müller 2019](#)), distribution of image features from head CT scans ([Salazar et al. 2020](#)), distributions of stock return ([Harvey et al. 2016](#), [Bekierman & Gribisch 2021](#), [Zhang et al. 2022](#)), the age distribution of fertility rates ([Mazzuco & Scarpa 2015](#)) and age distribution of life-table death counts in demography ([Bergeron-Boucher et al. 2017](#)).

To model density-valued functional data, [Jones & Rice \(1992\)](#) estimated density function by kernel density estimator and displayed density function via principal components. [Nerini & Ghattas \(2007\)](#) proposed regression trees where the response variable is PDFs. [van der Linde \(2008\)](#)

introduced Bayesian functional principal component analysis and applied it to simulated data consisting of nonparametric density estimates. [Srivastava et al. \(2011\)](#) proposed a time-warping function where the square root transformation of densities resides in the Hilbert space. [Dai \(2022\)](#) considered statistical inference of the Fréchet mean on the Hilbert sphere with application to random densities. [Zhang et al. \(2022\)](#) proposed Wasserstein autoregressive models for density time series. [Shang & Haberman \(2020, 2025a,b\)](#) considered the center log-ratio transformation,

While any PDF f may be thought of as random element of a Hilbert space, it does not reside in linear space due to summability and non-negativity constraints (i.e. $f \geq 0$ and $\int f = 1$); if f, g are two PDFs and a, b two real values, then the combination $a f + b g$ is not a PDF anymore. Consequently, the standard space of square-integrable functions \mathcal{L}^2 is not the most appropriate for representing PDFs. A natural way to deal with such constraints is to peel them away by an invertible transformation that maps densities onto a linear space. From an extrinsic viewpoint, such transformations include the Bayes Hilbert space approach (see, e.g., [Hron et al. 2016](#), [Menafoglio et al. 2022](#)), compositional data analysis (CoDa) ([Shang & Haberman 2020](#)), cumulative distribution function transformation ([Shang & Haberman 2025a](#)), α transformation ([Shang & Haberman 2025b](#)) and log quantile density transformation (LQDT) (see, e.g., [Petersen & Müller 2016](#), [Han et al. 2020](#)). [Kokoszka et al. \(2019\)](#) compared the finite-sample performance of density estimation and forecasting among the LQDT, CoDa, unconstrained functional principal component regression of [Horta & Ziegelmann \(2018\)](#), and a skewed- t distribution of [Wang \(2012\)](#). [Kokoszka et al. \(2019\)](#) recommended the LQDT and CoDa, two benchmark methods in our empirical studies.

In this paper, we focus on a random process taking values in some space of densities. We aim to forecast nonparametrically a future density given those observed in the past. Density forecasting is of great importance, especially in demography. In the realm of actuarial statistics, an important use of density forecasting is to predict the age distribution of life-table death counts as a means of computing survival probabilities. In such a model, any wrong specification of the forecast density may produce an inaccurate estimate of value-at-risk and make the asset holder, i.e., insurance companies, unable to control risk (see, e.g., [Shang 2013](#)). In [Figure 1](#), we present a time series of age-specific life-table death counts for the United States of America (USA) from 1933 to 2023 obtained from the [Human Mortality Database \(2025\)](#).

This setting faces three non-standard frameworks: 1) nonparametric density-on-density regression, 2) the dependency of the sequence of observed density functions, and 3) the convexity

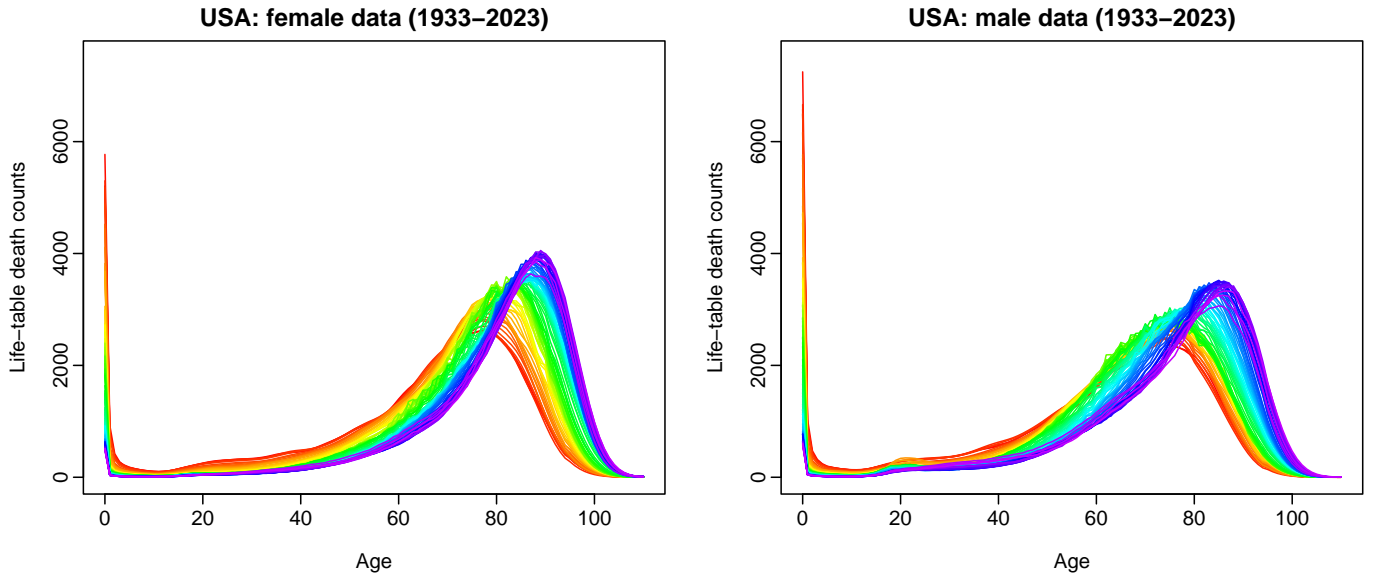


Figure 1 Rainbow plots of the age distribution of life-table death count from 1933 to 2023 in a single-year group. The life-table radix is 100,000 for each year. The life-table death counts in the oldest years are shown in red, while the most recent years are in violet. Curves are ordered chronologically according to the colours of the rainbow.

property of the space of densities that do not form a linear space. To take into account the nonlinear feature of the space of PDFs, we consider the Bayes Hilbert space approach (see, e.g., [Egozcue et al. 2006](#), [Van den Boogaart et al. 2010, 2014](#), [Hron et al. 2016](#)). The Bayes Hilbert spaces provide a mathematical environment allowing the extension of the Aitchison geometry from finite-dimensional compositional data ([Aitchison 1986](#), [Pawlowsky-Glahn et al. 2015](#)) to an infinite-dimensional setting. The Bayes Hilbert space is a linear space of PDFs designed for statistical models involving random PDFs (see, e.g., [Delicado 2011](#), [Hron et al. 2016](#), [Seo & Beare 2019](#), [Joen & Park 2020](#)).

A nonparametric density-on-density regression, where the response is one step ahead of the predictor in a time series of densities, is defined in the Bayes Hilbert space. A distance-based approach with a kernel-type estimator is proposed. Its flexibility makes the implementation attractive as various distance metrics may be considered. Its simplicity also makes the implementation easy and computationally fast as it does in the more standard nonparametric function-on-function regression setting (see, e.g., [Ferraty et al. 2012](#), [Lian 2012](#)). The advantage of nonparametric modelling is to capture the possible nonlinear dependence between two consecutive random PDFs. Unfortunately, instead of observing the density-valued random process, we sometimes only have samples drawn from these density functions (see also [Kokoszka et al. 2019](#), [Shang & Haberman 2020](#), [Zhang et al. 2022](#)). This is why our methodology often includes, in its first step, the estimation of the densities before estimating the nonparametric relationship between densities.

The paper is organised as follows. Section 2.1 reminds the basic geometrical concepts of Bayes Hilbert space. In Section 2.2, we describe a model, estimation and forecasting scheme for our nonparametric density-on-density regression. In Section 2.3, we present asymptotic properties associated with our Bayes Nadaraya-Watson (NW) estimator. In Section 3.1, we describe how we estimate density via a kernel density estimator, the selection of optimal bandwidth, and the criterion used to assess density estimation accuracy. In Section 3.2, we evaluate and compare our Bayes NW estimator in the nonparametric density-on-density regression via a series of simulation studies. A French COVID19 hospitalisation data analysis is shown in Section 3.3, and a data analysis of age-specific life-table death count in the United States (U.S.) is presented in Section 3.4. The conclusion is given in Section 4, along with some ideas on how the methodology can be further extended.

2 Nonparametric density-on-density regression

We first briefly remind the definition of the Bayes Hilbert space before introducing the density-on-density regression model. It is essential to understand how this vector space of PDFs works and its associated geometry.

2.1 Bayes Hilbert space: a vector space of PDFs

Bayes Hilbert space. Let $\mathcal{B}^2(I)$ be the set of bounded PDFs f with continuous support $I = [a, b]$ for which the natural logarithm is square integrable:

$$\mathcal{B}^2(I) = \left\{ f : I \mapsto]0, +\infty[, \int_I f = 1, \int_I \{\ln(f)\}^2 < +\infty \right\}.$$

Remark: to simplify notations, when there is no ambiguity, arguments of integrand are forgotten. Two fundamental operators \oplus and \odot respectively called *perturbation* and *powering* are defined for any f, g in $\mathcal{B}^2(I)$ and r in \mathbb{R} :

$$(f \oplus g)(t) = \frac{f(t)g(t)}{\int_I f(u)g(u) du}, \quad (r \odot f)(t) = \frac{f^r(t)}{\int_I f^r(u) du}.$$

The perturbation is commutative and associative:

$$f \oplus g = g \oplus f, \quad (f \oplus g) \oplus h = f \oplus (g \oplus h).$$

Let $\mathbf{0}_B = \frac{1}{b-a}1_I$, the uniform PDF defined on I , is the neutral element ($f \oplus \mathbf{0}_B = \mathbf{0}_B \oplus f = f$) for perturbation and f^{-1} is the unique element such that $f \oplus f^{-1} = f^{-1} \oplus f = \mathbf{0}_B$. The power is associative ($r \odot (s \odot f) = (rs) \odot f$), distributive with respect to perturbation ($r \odot (f \oplus g) = (r \odot f) \oplus (r \odot g)$) and scalar addition ($(r+s) \odot f = (r \odot f) \oplus (s \odot f)$), and 1 is its neutral element. Based on the perturbation and powering, a third operator \ominus called *perturbation-substraction* is defined:

$$f \ominus g = f \oplus (-1) \odot g.$$

In $\mathcal{B}^2(I)$, the inner product is defined as:

$$\langle f, g \rangle_B = \frac{1}{2(b-a)} \int_I \int_I \ln \frac{f(u)}{f(v)} \ln \frac{g(u)}{g(v)} du dv$$

and one has useful properties: 1) $(\mathcal{B}^2(I), \oplus, \odot, \langle \cdot, \cdot \rangle_B)$ is a vector space, 2) $(\mathcal{B}^2(I), \oplus, \odot, \langle \cdot, \cdot \rangle_B)$ forms a separable Hilbert space called Bayes Hilbert space (see [Egozcue et al. 2006](#), [Van den Boogaart et al. 2014](#)). At last, for any f, g in $\mathcal{B}^2(I)$, $\|f\|_B = \sqrt{\langle f, f \rangle_B}$ is the norm associated with the inner product. One can remark that $\|f \ominus g\|_B = 0$ is equivalent to $f \ominus g = \mathbf{0}_B$, which results in $f(u) = g(u)$ for any $u \in I$.

Isometry between $\mathcal{B}^2(I)$ and $\mathcal{L}_0^2(I)$. Let $\mathcal{L}_0^2(I)$ be the space of square-integrable real functions f on I with $\int_I f = 0$. There exists an isometric isomorphism between $\mathcal{B}^2(I)$ and $\mathcal{L}_0^2(I)$ called centered log-ratio (clr) transformation, defined for any PDF f in $\mathcal{B}^2(I)$ and any u in I :

$$\text{clr}(f)(u) = \ln f(u) - (b-a)^{-1} \int_I \ln f.$$

In addition of the isometry property of the clr transformation $\|f \ominus g\|_B = \|\text{clr}(f) - \text{clr}(g)\|$ where $\|g\| = \int_I g^2$, $\text{clr}(f \oplus g) = \text{clr}(f) + \text{clr}(g)$, $\text{clr}(s \odot f) = s \times \text{clr}(f)$, and its inverse transformation

$$\text{clr}^{-1}(g) = \frac{\exp(g)}{\int_I \exp(g)},$$

for any g in $\mathcal{L}_0^2(I)$.

Once the Bayes Hilbert space framework is reminded, one can introduce our nonparametric density-on-density regression when considering a time series of PDFs.

2.2 Model, estimation, and sequential forecasting scheme

2.2.1 Density-on-density regression model

Let $\{\mathcal{F}_t\}_{t \in \mathbb{Z}}$ be a stochastic process taking values in $\mathcal{B}^2(I)$ and consider $N + 1$ random PDFs (f_1, \dots, f_{N+1}) as realizations of $(\mathcal{F}_1, \dots, \mathcal{F}_{N+1})$. The main goal is to forecast a future PDF f_{N+2} given those observed in the past $(f_{N+1}, f_N, \dots, f_1)$. To this end, we propose the nonparametric density-on-density regression model

$$f_{t+1} = m(f_t) \oplus \epsilon_t, \quad t = 1, \dots, N, \quad (1)$$

where $m(\cdot)$ is an unknown smooth operator mapping $\mathcal{B}^2(I)$ into $\mathcal{B}^2(I)$, and for each t , $E(\epsilon_t | f_t) = \mathbf{0}_{\mathcal{B}}$, where the conditional expectation is defined for $\mathcal{B}^2(I)$ -valued random PDFs. The definition of conditional expectation for Hilbert-valued random variable can be found in [Bosq \(2000\)](#). Under Model (1), it is easy to check that, for each t , $E(\epsilon_t | f_t) = \mathbf{0}_{\mathcal{B}}$ is equivalent to $m(f) = E(f_{t+1} | f_t = f)$ (see Section A in Appendix). Our main challenge is to define for any given density f an estimator $\tilde{m}(f)$ of the unknown regression operator $m(f) = E(f_{t+1} | f_t = f)$ fulfilling density features (nonnegative functions that integrate to one) and good asymptotic behaviour while no reducing functional form (i.e. linearity, additivity, functional index model, etc) of the unknown regression operator $m(\cdot)$ is assumed.

2.2.2 Kernel estimator

With some smoothness properties, the functional form of $m(\cdot)$ is often estimated in a data-driven manner. There are a number of nonparametric functional estimators, such as functional Nadaraya-Watson (NW) estimator ([Ferraty & Vieu 2006](#)), functional local linear estimator ([Berliner et al. 2011](#), [Ferraty & Nagy 2022](#)), functional k -nearest neighbour estimator ([Burba et al. 2009](#), for scalar response and [Lian 2011](#), for functional response), functional smoothing splines ([Crainiceanu & Goldsmith 2010](#)), functional wavelet estimator ([Antoniadis & Sapatinas 2003](#)), distance-based local linear estimator ([Boj et al. 2010](#)) and functional neural network ([Rossi & Villa 2006](#)). Throughout

the paper, we introduce the functional Bayes NW estimator, i.e., the functional NW estimator in the Bayes-Hilbert space, because of its simplicity and mathematical elegance. The essence of functional Bayes NW kernel smoothing is to allow flexible estimation of the unknown regression operator. The functional Bayes NW estimator of the conditional mean can be defined as

$$\tilde{m}_N(f) = \bigoplus_{t=1}^N w_{h_r}(f_t, f) \odot f_{t+1} \quad \text{with} \quad w_{h_r}(f_t, f) = \frac{K_r(h_r^{-1} \|f_t \ominus f\|_{\mathcal{B}})}{\sum_{t=1}^N K_r(h_r^{-1} \|f_t \ominus f\|_{\mathcal{B}})}, \quad (2)$$

where $K_r(\cdot)$ is an asymmetric kernel function and h_r is a positive smoothing parameter (i.e. bandwidth). The vector space property of $\mathcal{B}^2(I)$ ensures that the Bayes NW estimator is a PDF. Depending on the kernel function and bandwidth parameter, the nonparametric estimator in (2) is a weighted average of the observed densities and has two interesting properties: it fulfils the PDF constraints by construction, and due to its simplicity, its implementation is straightforward and computationally fast.

In practice, conditionally on the densities f_1, \dots, f_{N+1} , we observe n_t copies $X_{t,1}, \dots, X_{t,n_t}$ that share the same marginal density f_t for each $t = 1, \dots, N + 1$. In other words, the PDFs are not directly observable. This situation is particularly common in epidemiology. For instance, suppose that at each date t , COVID-19 confirmed cases corresponding to ω French departments are observed. In this case, $X_{t,j}$ is the COVID-19 confirmed cases at date t of the department j and all the sample sizes are equal ($n_1 = n_2 = \dots = \omega$). This is why our methodology first focuses on kernel estimators $\hat{f}_1, \dots, \hat{f}_{N+1}$ of the $N + 1$ probability densities f_1, \dots, f_{N+1} . In the second step, we just plug the estimated densities $\hat{f}_1, \dots, \hat{f}_{N+1}$ into the nonparametric density-on-density regression estimator (2) which provides our definitive kernel estimation:

$$\hat{m}_N(f) = \bigoplus_{t=1}^N w_{h_r}(\hat{f}_t, f) \odot \hat{f}_{t+1},$$

where $w_h(\hat{f}_t, f)$ is defined in (2). A standard by-product of this estimating procedure in the time series context is the following one-step-ahead sequential forecasting scheme. From the estimated density functions $\hat{f}_1, \dots, \hat{f}_{N+1}$, we compute $\hat{f}_{N+2} = \hat{m}_N(\hat{f}_{N+1})$ which is the prediction of the density f_{N+2} . To forecast the next density, just consider the sample of random densities completed with the predicted one (i.e. $\hat{f}_1, \dots, \hat{f}_{N+1}, \hat{f}_{N+2}$) and build $\hat{f}_{N+3} = \hat{m}_{N+1}(\hat{f}_{N+2})$. This one-step-ahead forecasting scheme can be iterated to get $\hat{f}_{N+\mathcal{H}}$ at any reasonable forecast horizon \mathcal{H} .

2.2.3 Dependence model

To better understand the dependence structure of our data, our framework combines two random mechanisms: 1) the underlying process $\{\mathcal{F}_t\}_{t \in \mathbb{Z}}$ generating the random PDFs $\{f_1, \dots, f_{N+1}\}$ and 2) the random process providing the $N + 1$ samples $\{X_{t,1}, \dots, X_{t,m_t}\}_{t=1, \dots, N+1}$ for estimating the non-observable random PDFs. For any $t = 1, 2, \dots, N$, set $\mathbf{X}_t = \{X_{t,1}, \dots, X_{t,m_t}\}$; the scheme hereafter sums up the overall random situation:

$$\begin{array}{ccccccc}
 \text{Density-valued process} & f_1 & \longrightarrow & f_2 = m(f_1) \oplus \epsilon_1 & \longrightarrow & \cdots & \longrightarrow & f_{N+1} = m(f_N) \oplus \epsilon_N \\
 & \downarrow & & \downarrow & & & & \downarrow \\
 \text{Observed data} & \mathbf{X}_1 & & \mathbf{X}_2 & & & & \mathbf{X}_{N+1} \\
 & \downarrow & & \downarrow & & & & \downarrow \\
 \text{Estimated densities} & \hat{f}_1 & & \hat{f}_2 = \hat{m}_N(\hat{f}_1) & & & & \hat{f}_{N+1} = \hat{m}_N(\hat{f}_N)
 \end{array}$$

We assume that the random process of two consecutive densities $\{(\mathcal{F}_t, \mathcal{F}_{t+1})\}_{t \in \mathbb{Z}}$ is a strictly stationary ρ -mixing process (see, e.g., [Rio 1993](#), [Bradley 2005](#)). We first remind the definition of the ρ -mixing dependence condition. For any σ -field \mathcal{A} , let $\mathcal{L}^2(\mathcal{A})$ denote the space of square-integrable \mathcal{A} -measurable real-valued random variables. Given two σ -fields \mathcal{A} and \mathcal{B} , $\rho(\mathcal{A}, \mathcal{B}) = \sup \{ |\text{Corr}(U, V)|, U \in \mathcal{L}^2(\mathcal{A}), V \in \mathcal{L}^2(\mathcal{B}) \}$ measures the dependence between \mathcal{A} and \mathcal{B} in terms of correlation. ρ is between 0 and 1; the closer this quantity is to 0, the weaker the dependency. Let $\{\mathcal{Z}_t\}_{t \in \mathbb{Z}}$ be a random process and for any $k < \ell$, define \mathcal{A}_k^ℓ as the σ -field generated by the \mathcal{Z}_t 's for t between k and ℓ . The random sequence $\{\mathcal{Z}_t\}_{t \in \mathbb{Z}}$ is said to be ρ -mixing if the dependence coefficients $\rho(m) = \sup_{j \in \mathbb{Z}} \rho(\mathcal{A}_{-\infty}^j, \mathcal{A}_{j+m}^{+\infty})$ tends to 0 as m goes to infinity. This asymptotic property is usually called the ρ -mixing condition. Assuming that $\{(\mathcal{F}_t, \mathcal{F}_{t+1})\}_{t \in \mathbb{Z}}$ is ρ -mixing is equivalent to suppose that its dependence coefficients fulfill the ρ -mixing condition with $\mathcal{Z}_t = (\mathcal{F}_t, \mathcal{F}_{t+1})$. Then, according to the scheme generating the data, it is reasonable to suppose that the random sequences $(f_t, f_{t+1})_{t=1,2,\dots}$ and $(\mathbf{X}_t, \mathbf{X}_{t+1})_{t=1,2,\dots}$ inherit the structure (i.e strictly stationary and ρ -mixing) of $\{(\mathcal{F}_t, \mathcal{F}_{t+1})\}_{t \in \mathbb{Z}}$. As a by-product, the random sequence $(\hat{f}_t, \hat{f}_{t+1})_{t=1,2,\dots}$ based on the estimated densities is also a strictly stationary ρ -mixing process. Lastly, to complete the structure of our data, conditionally to f_t and for each $t = 1, \dots, N$, the error model ϵ_t is assumed independent of \mathbf{X}_t .

2.3 Asymptotic properties

This section is devoted to the theoretical properties of our density's functional kernel estimator. We first introduce notations and assumptions we need to derive the asymptotic behaviour of $\widehat{m}(f)$.

(H1) It exists $C > 0$ such that, for all f and g in $\mathcal{B}^2(I)$, $\|m(f) \ominus m(g)\|_{\mathcal{B}} \leq C \|f \ominus g\|_{\mathcal{B}}$,

(H2) it exists $a > 1$ such that the ρ -mixing coefficient fulfills the condition $\rho(k) = O(k^{-a})$,

(H3) set $n = \inf_{t \geq 1} n_t$ and let $n = n_N$ be a sequence depending on N such that n goes to infinity with N ; one assumes the existence of a sequence δ_N tending to 0 as N goes to infinity such that, for any t , $E \left(\|\widehat{f}_t \ominus f_t\|_{\mathcal{B}}^2 \right) = O(\delta_N^2)$,

(H4) For any deterministic f in $\mathcal{B}^2(I)$, set $\pi_f(h_r) = P(\|f_1 \ominus f\|_{\mathcal{B}} < h_r)$; it exists $C > 0$ and $C' > 0$, $0 < C\pi_f(h_r) \leq \pi_f(h_r + o(h_r)) \leq C'\pi_f(h_r)$,

(H5) h_r tends to 0 with N , $N^{a/(1+a)} \pi_f(h_r)$ goes to infinity with N , and it exists b with $1/3 < b < 1$ such that $\delta_N^{2b} = o(\pi_f(h_r))$ and $\delta_N^{1-b} = o(h_r)$,

(H6) K_r asymmetric Lipschitz kernel with support $[0, 1]$ such that $\exists C$ and C' , $0 < C 1_{[0,1]} \leq K_r \leq C' 1_{[0,1]}$.

(H1) is usual; it requires that the regression operator is smooth enough by fulfilling the Lipschitz property. In (H2), the model dependency assumes an arithmetic decay for the mixing coefficients. This assumption simplifies the convergence rate, but more general writing involving the mixing coefficients $\rho(N)$ can be obtained. (H3) relates, for each t , the size n_t of the sample $X_{t,1}, \dots, X_{t,n_t}$ to the number N of random PDFs. In addition, it requires that the mean integrated squared error $E \left(\|\widehat{f}_t \ominus f_t\|_{\mathcal{B}}^2 \right)$ of \widehat{f}_t tends to zero when n_t (i.e. N) goes to infinity. In the standard multivariate setting, the sequence δ_N can be interpreted as an upper bound of the well-known quantity $\text{MISE}(\widehat{f}_t) = E \left(\|\widehat{f}_t - f_t\| \right)$ (for more details on MISE, see [Rosenblatt 1956](#), [Epanechnikov 1969](#), [Wegman 1972](#), [Nadaraya 1974](#), [Marron & Wand 1992](#), [Hansen 2005](#), among others). It is shown Section A in Appendix that as soon as $f \in \mathcal{B}^2(I)$ with $f \geq \theta > 0$, $E \left(\|\widehat{f}_t \ominus f_t\|_{\mathcal{B}}^2 \right) = O \left\{ \text{MISE}(\widehat{f}_t) \right\}$. In other words, when the density f admits a strictly nonnegative lower bound, then $E \left(\|\widehat{f}_t \ominus f_t\|_{\mathcal{B}}^2 \right)$ inherits the asymptotic properties of MISE. The hypothesis (H4) assumes that the behaviour of the small ball probability $\pi_f(h)$ is not sensitive to variations on radius negligible with respect to the bandwidth h (see [Li & Shao 2001](#) for a survey on small ball probability). According to the isometry

property of the clr transformation (see Section 2.1), $\pi_f(h_r) = P(\|X - x\|_2 < h_r)$ with $X = \text{clr}(f_1)$ and $x = \text{clr}(f)$ in $\mathcal{L}_0^2(I)$; the class of $\mathcal{L}_0^2(I)$ -valued random functions fulfilling (H4) encompasses Gaussian-type random processes (see Ferraty et al. 2019). (H5) relates the asymptotic behaviour of h_r , $\pi_f(h_r)$, N and δ_N^2 , the upper bound of $E\left(\|\widehat{f}_t \ominus f_t\|_{\mathcal{B}}^2\right)$ for any t . As $\pi_f(h_r)$ tends to zero with N faster than h_r does, it is reasonable to require that $2b > 1 - b > 0$ which results in $1/3 < b < 1$. With (H6) and for any $q > 0$, $E\{K_r^q(h^{-1}\|f_t \ominus f\|_{\mathcal{B}})\}$ is bounded below and above by a quantity of order $\pi_f(h_r)$. For simplicity, we use a basic hypothesis on the kernel function. Nevertheless, it is possible to get the more accurate result $E\{K_r^q(h_r^{-1}\|f_t \ominus f\|_{\mathcal{B}})\} = C_{f,q}\pi_f(h_r)\{1 + o(h_r)\}$ as soon as the kernel function K_r is continuously differentiable on $(0, 1)$ with $K_r(1) > 0$, and for all $s \in (0, 1)$, $K_r'(s) \leq 0$ and the ratio $\pi_f(h_r s)/\pi_f(h_r)$ tends to some positive value as h tends to 0.

Once notations and assumptions are introduced, one can provide our main result by giving the pointwise convergence rate of our density-on-density kernel regression estimator; the proof is postponed to Section B of the Appendix.

THEOREM 1 *If (H1)-(H6) are fulfilled, then*

$$\|\widehat{m}_N(f) \ominus m(f)\|_{\mathcal{B}} = O(h_r) + O\left(\delta_N \pi_f(h_r)^{-1/2}\right) + O_P\left(\left\{N^{a/(1+a)} \pi_f(h_r)\right\}^{-1/2}\right).$$

The first two terms correspond to the bias part. $O(h_r)$, which is not surprising (see Ferraty & Vieu 2006), is derived from the regularity assumption acting on the regression operator m (see (H1)). The second term, which is not usual, involves δ_N and the small ball probability $\pi_f(h_r)$. This is the price to pay when the random PDFs are not directly observed and are approximated by means of some estimating procedure, where δ_N can be interpreted as the upper bound of the root MISE of \widehat{f}_t for any t . For the variance part, remember that a controls the asymptotic behaviour of the mixing coefficient. So, the impact of the dependency model appears directly in the exponent of the sample size N of the random densities. In the situation of a sample of independent explanatory functional random variables, we would get N instead of $N^{a/(1+a)}$ (see again Ferraty & Vieu 2006). As expected, the dependence structure of the data degrades the rate of convergence of \widehat{m} .

Let us now focus on the estimation of the random density f_t with a particular attention on the sequence δ_N which is an upper bound of $\text{MISE}(\widehat{f}_t)$. The more standard situation corresponds to the observation of an independent and identically distributed (iid) sample $X_{t,1}, \dots, X_{t,n_t}$ but dependent data received also lots of attention (see Rosenblatt 1971, Nadaraya 1974, Chanda 1983,

Hart 1984, Castellana & Leadbetter 1986, Robinson 1986, Hall & Hart 1990, Chesneau 2014, among others). In the special case of a kernel density estimator

$$\hat{f}_t(x) = (n_t h_t)^{-1} \sum_{i=1}^n K_d \left\{ h_t^{-1}(x - X_{t,i}) \right\},$$

with h_t a bandwidth tending to zero when n_t goes to infinity and K_d a kernel function, the asymptotic behaviour of $\text{MISE}(\hat{f}_t)$ is well known, even when the data $X_{t,1}, \dots, X_{t,n_t}$ come from a stationary strong mixing process. When f_t is deterministic, Biau (2002) stated that the asymptotic behaviour of $\text{MISE}(\hat{f}_t)$ for dependent observations (with arithmetic decay rate for the mixing coefficient) is the same than those obtained for independent data: $\text{MISE}(\hat{f}_t) = O(h_t^4) + O(n_t^{-1}h_t^{-1})$. Setting $h_t \sim n_t^{-1/5}$ in order to balance both terms results in $\text{MISE}(\hat{f}_t) = O(n_t^{-4/5})$. This result requires that the first two derivatives f_t' and f_t'' of the true density function f_t are continuous with $\int (f_t'')^2 < \infty$. When f_t is a random density, one can write $\text{MISE}(\hat{f}_t) = \mathbb{E} \left\{ \mathbb{E} \left(\|\hat{f}_t - f_t\|^2 | f_t \right) \right\}$. Then, it is easy to see that the same result holds as soon as

$$(H7) \quad f_1' \text{ and } f_1'' \text{ are continuous almost surely with } \mathbb{E} \left\{ \int (f_1'')^2 \right\} < \infty.$$

The following result simplifies the rate of convergence given in THEOREM 1 when the random densities are estimated with the kernel density estimator.

COROLLARY 1 *If, in addition of (H1)-(H7), one has*

(H8) $X_{t,1}, \dots, X_{t,n_t}$ are iid or generated from a stationary ρ -mixing process with arithmetic decay rate for the mixing coefficients,

(H9) for any t , it exists $q > 5a / \{4b(1+a)\}$ such that $n_t \sim N^q$ and $h_t \sim N^{-q/5}$,

Then

$$\|\hat{m}_N(f) \ominus m(f)\|_{\mathcal{B}} = O(h_r) + O_P \left(\left\{ N^{a/(1+a)} \pi_f(h_r) \right\}^{-1/2} \right).$$

(H9) corresponds to a particular case where δ_N^2 , the upper bound of $\mathbb{E} \left(\|\hat{f}_t \ominus f_t\|_{\mathcal{B}}^2 \right)$, is negligible with respect to $N^{-a/(1+a)}$ so that the term $O \left(\delta_N \pi_f(h_r)^{-1/2} \right)$ vanishes.

3 Finite-sample properties

3.1 Implementation

Since the actual densities in practical applications are not often observable, we work with densities which are outputs of kernel density estimators:

$$f_t(u) = \frac{1}{n_t h_t} \sum_{i=1}^{n_t} K\left(\frac{u - X_{t,i}}{h_t}\right), \quad t = 1, \dots, n, \quad (3)$$

where $K(\cdot)$ denotes a kernel function and h_t denotes a bandwidth for period t . We consider the truncated Gaussian kernel.

In our nonparametric density-on-density regression, we consider how to select the optimal bandwidths for estimating the nonparametric regression operator in (1) and for estimating densities in (3). To estimate densities from observed data, we use a kernel density estimator with the bandwidth selected by Silverman's rule-of-thumb (ROT) (see also Kokoszka et al. 2019). Kokoszka et al. (2019) used Silverman's ROT to select the bandwidth, which leads to $\hat{h}_t = 2.34 \times \hat{\sigma}_t \times n_t^{-1/5}$, where $\hat{\sigma}_t$ denotes the sample standard deviation of the returns $X_{t,i}$, $i = 1, \dots, n_t$.

To estimate the bandwidth for the nonparametric regression operator, we can use generalised cross-validation (GCV) to select the bandwidth automatically (see, e.g., Ferraty et al. 2012). The GCV aims to minimise an overall squared loss function between the estimated and observed responses among the data in the training sample.

3.2 Monte-Carlo simulation studies

We conduct a series of simulation studies to examine the finite-sample performance of the nonparametric density-on-density regression described in Section 2. Our data generating process consists of the following steps:

- 1) When generating the model $f_{t+1} = m(f_t) \oplus \epsilon_t$, a first step is to be able to simulate $\epsilon_0, \epsilon_1, \dots$, the probability density functions playing the role of model errors. By using the clr transformation, the density-on-density regression model is equivalent to $\text{clr}(f_{t+1}) = \text{clr} \circ m(f_t) + \text{clr}(\epsilon_t)$. Instead of generating directly the errors ϵ_t in the Bayes Hilbert space $\mathcal{B}^2(I)$, it could be more convenient to simulated functional errors $\eta_t = \text{clr}(\epsilon_t)$ in the corresponding Hilbert space $\mathcal{L}_0^2(I)$.

2) According to the properties of the clr transformation and the zero-mean constraint in $\mathcal{B}^2(I)$ of ϵ_t given f_t , the model error η_t has to fulfill two constraints: $E(\eta_t|f_t) = 0$, and for all $u \in I$, $\int_I \eta_t(u) du = 0$. A way to generate such η_t 's is to use the trigonometric functions ϕ_1, ϕ_2, \dots defined on $I = [-1, 1]$: $\forall k = 1, 2, \dots$, $\phi_{2k-1}(u) = \cos(k\pi u)$ and $\phi_{2k}(u) = \sin(k\pi u)$. One can remark that the ϕ_k 's integrate to 0 for any non-null integer k . For any $u \in [-1, 1]$, and any subset \mathcal{K} of nonnull integers, set

$$\eta_t(u) = \sum_{k \in \mathcal{K}} A_{tk} \phi_k(u).$$

If $E(A_{tk}|f_t) = 0$, then $E(\eta_t|f_t) = 0$ and the integral property of the Fourier basis elements results in $\int_{-1}^1 \eta_t(u) du = 0$. For instance, one can set

$$\eta_t(u) = A_{t1} \cos(\pi u) + A_{t2} \sin(\pi u) + A_{t3} \cos(2\pi u) + A_{t4} \sin(2\pi u) + A_{t5} \cos(3\pi u),$$

where A_{tj} 's are iid zero-mean real random variables (r.r.v.). In Figure 2, we present such model errors η_t with $A_{t1}'s, \dots, A_{t5}'s \stackrel{iid}{\sim} N(0, \sigma^2)$.

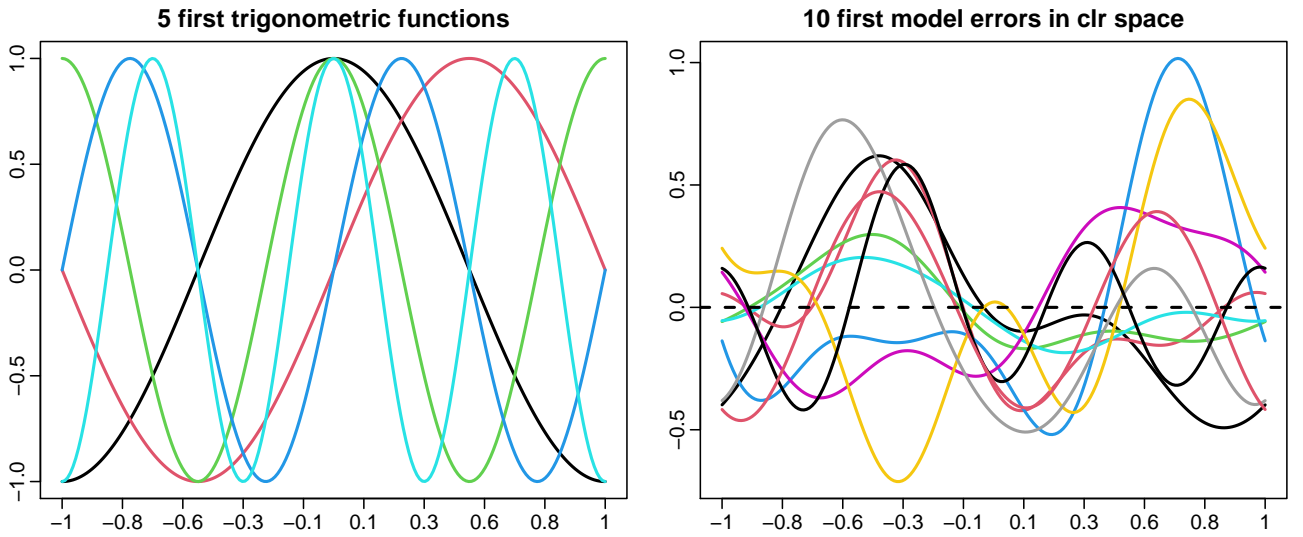


Figure 2 The basis functions we considered are the first five trigonometric functions. By multiplying them with random coefficients simulated from a Gaussian distribution, we obtain the model error in the clr space, $\eta_t(u)$.

Transform back to ϵ_t 's with the inverse of the clr transformation: $\epsilon_t = \text{clr}^{-1}(\eta_t)$. In Figure 3, we present 10 first model errors in Bayes space.

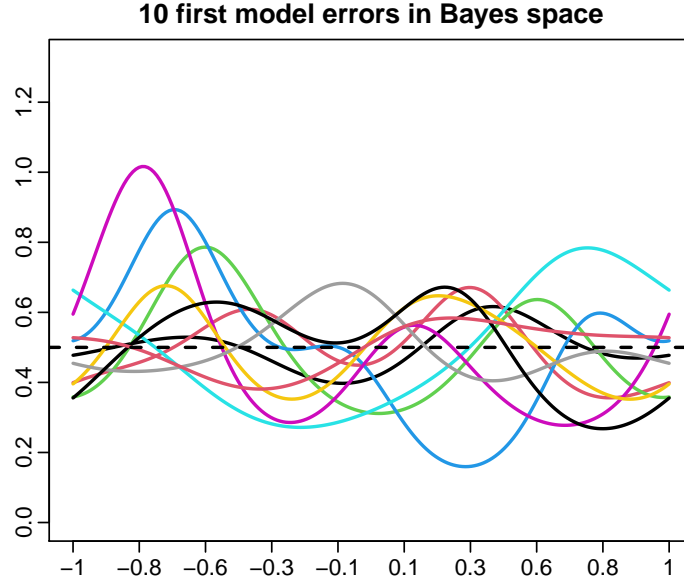


Figure 3 By taking the inverse clr transformation of the model error in Figure 2, we obtain the model error in Bayes space.

3) Let us define the regression operator $m : \mathcal{B}^2(I) \rightarrow \mathcal{B}^2(I)$ such that

$$m(f)(y) = (1 - \rho_0)^{-1} \left\{ \int_{\underline{b}}^{\bar{b}} f(x) g \left(\frac{y - \rho_0 x}{1 - \rho_0} \right) dx \right\} 1_{[-1,1]}(y)$$

with f and g two given probability densities in $\mathcal{B}^2(I)$, $0 < \rho_0 < 1$ and where $\underline{b} = \max[-1, \rho_0^{-1}(y + \rho_0 - 1)]$ and $\bar{b} = \min[1, \rho_0^{-1}(y - \rho_0 + 1)]$. Depending on the value of ρ_0 , the function support may vary for the regression mean function. This regression operator has a nice interpretation in terms of convolution. Suppose that, for any $0 < \rho_0 < 1$, $Z = \rho_0 X + (1 - \rho_0)Y$ with X and Y two independent r.r.v. and let f_Z (resp. f_X) be the PDF of Z (resp. X). Then, we have $f_Z = m(f_X)$ and $\text{Corr}(Z, X) = \rho_0$. The regression operator $m(\cdot)$ corresponds to the transformation resulting from a convex combination of X with another r.r.v. Y . Based on this remark, we propose the following scheme for simulating our time series of PDFs in the Bayes Hilbert space:

$$f_{t+1} = m(f_t) \oplus \epsilon_t,$$

where the ϵ_t 's are the model errors in Bayes space (built previously): 1) $m(f_t)$ represents the PDF of $X_{t+1} = \rho_0 X_t + (1 - \rho_0)Y_{t+1}$ when f_t is the PDF of X_t , 2) f_{t+1} is the obtained PDF when adding some model error ϵ_t to $m(f_t)$.

4) Set $Y_t \sim g_t = TN(\mu_t, \nu^2)$ where $TN(\mu_t, \nu^2)$ is the truncated normal distribution over $[-1, 1]$ derived from the normal distribution $N(\mu_t, \nu^2)$ where, for some constant $T > 0$, $\mu_t =$

$\cos(2\pi t/T)$.

- 5) Set $f_1 \equiv g_1$ where $g_1 = TN(\mu_1, \nu^2)$ with $\mu_1 = \cos(2\pi/T)$. We compute $f_2 = m(f_1) \oplus \epsilon_1$. Then, we iterate to build the whole time series of densities $f_1, f_2 = m(f_1) \oplus \epsilon_1, \dots, f_N = m(f_{N-1}) \oplus \epsilon_{N-1}$.

In Figure 4, we present a perspective plot of a simulated example with 150 curves. We consider 201 grid points within a function support range $[-1, 1]$. There are four tuning parameters to choose, namely σ in step 2), ρ_0 in step 3), ν and T in step 4). Let $\sigma = 0.1, \rho_0 = 0.5, \nu = 0.5$ and $T = 150$.

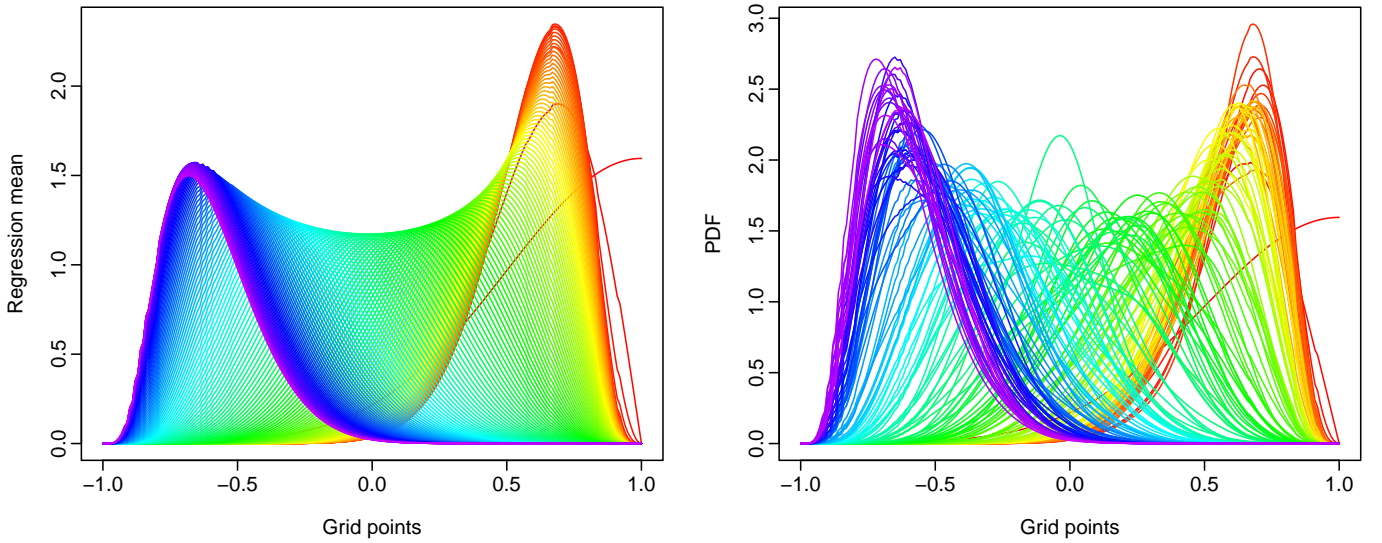


Figure 4 150 simulated densities with 201 grid points bounded between -1 and 1. The four tuning parameters are chosen as: $\sigma = 0.1, \rho = 0.5, \nu = 0.5$ and $T = 150$.

We divide the simulated data into a training sample and a testing sample comprised of the last 50 densities. To evaluate the finite-sample performance, we compute the Kullback-Leibler divergence (KLD) (Kullback & Leibler 1951). The KLD is intended to measure the loss of information when we choose an approximation. For two density functions, the discrete version of the Kullback-Leibler divergence is defined as

$$\text{KLD}_m = \frac{1}{50} \sum_{i=1}^{50} \left\{ D_{\text{KL}}[f_i^m(s) || \hat{f}_i^m(s)] + D_{\text{KL}}[\hat{f}_i^m(s) || f_i^m(s)] \right\}$$

$$\overline{\text{KLD}} = \frac{1}{100} \sum_{m=1}^{100} \text{KLD}_m,$$

where $f_i^m(s)$ is the i^{th} observation in the testing sample, and $\hat{f}_i^m(s)$ is the one-step-ahead forecast of $f_i^m(s)$ for the m^{th} replication.

For one out of 100 replications, we generate a sample of densities under different tuning parameters. With the training samples, we produce one-step-ahead forecast densities using the nonparametric density-on-density regression with the Bayes NW estimator, the CoDa method, the LQDT, and functional principal component regression of [Horta & Ziegelmann \(2018\)](#). In Figure 5, we present one replication of holdout densities and their forecasts obtained by the five methods. For this example, we observe that the nonparametric density-on-density regression produces the best results, followed closely by the random walk. The [Horta & Ziegelmann's \(2018\)](#) method suffers from the well-known tail problem when density forecasts can even be negative.

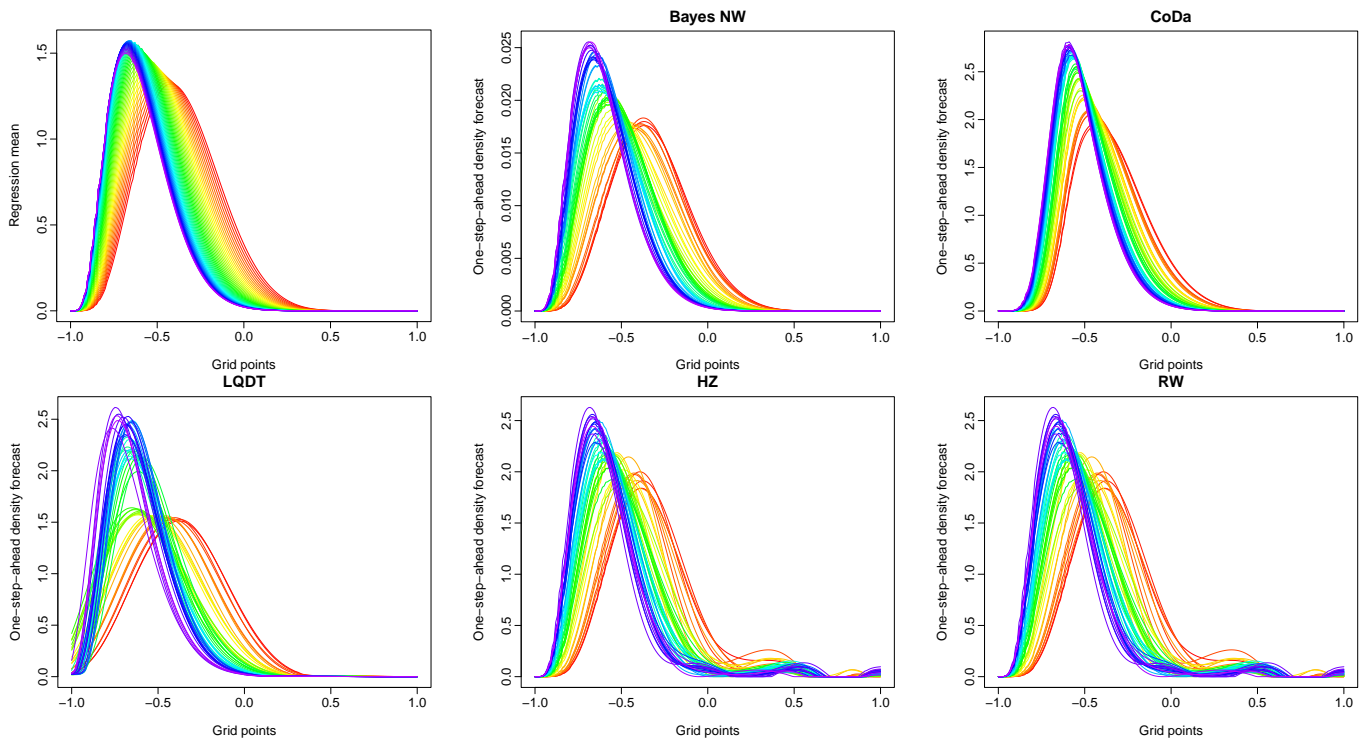


Figure 5 One simulated example with a sample size of $T = 150$ and 201 grid points between -1 and 1. While the first 100 densities are used as the initial training sample, we produce iterative one-step-ahead forecast densities via an expanding window scheme. HZ stands for [Horta & Ziegelmann's \(2018\)](#) method.

To further assess the overall forecast accuracy, we repeat the simulation data generating process 100 times, each with different pseudo-random seeds. In Table 1, we present the one-step-ahead averaged KLDs between the actual holdout samples and their corresponding forecasts obtained from the five methods. Further, we present results using expanding window approach where the size of the training samples increases. As measured by the $\overline{\text{KLD}}$ criterion, the forecast accuracy relies heavily on the noise-to-signal ratio, characterised by the dependence parameter ρ_0 and the standard deviation σ in the error term of the AR(1) structure. As the dependence parameter ρ_0 decreases from 0.75 to 0.25, we observe a decrease of $\overline{\text{KLD}}$ based on 100 replications. As the

standard deviation in the error term of the AR(1) structure increases from 0.1 to 1, we also observe an increase of $\overline{\text{KLD}}$. As the sample size increases from 150 to 550, we observe a general increase of $\overline{\text{nsr}}$ which does not translate to an increase of $\overline{\text{KLD}}$.

Table 1 One-step-ahead forecast accuracy of the nonparametric density-on-density regression with the Bayes NW estimator in the simulated data with 100 replications. We also compare the forecast accuracy with the CoDa, LQDT, HZ and RW methods, under three choices of (σ, ρ_0) with sample sizes of $T = 150, 350$ and 550 . The last 50 densities are the testing sample, while the remaining densities are the training sample. For the 100 replications, we compute the average noise-to-signal ratio, denoted by $\overline{\text{nsr}}$.

(σ, ρ_0)	n	$\overline{\text{nsr}}$	Method				
			Bayes NW	CoDa	LQDT	HZ	RW
(0.10, 0.75)	150	0.0398	0.0137	1.2085	3.7018	0.6377	0.0115
	350	0.0918	0.0079	0.4419	3.5817	0.0818	0.0108
	550	0.1439	0.0209	0.1213	0.0173	0.1772	0.0197
(0.10, 0.50)	150	0.0219	0.0069	0.1339	0.0880	0.0963	0.0097
	350	0.0353	0.0035	0.0593	0.0155	0.0389	0.0094
	550	0.0514	0.0082	0.0108	0.0119	0.0754	0.0125
(0.10, 0.25)	150	0.0272	0.0069	0.0170	0.2433	0.0628	0.0098
	350	0.0340	0.0016	0.0079	0.1584	0.0516	0.0098
	550	0.0434	0.0046	0.0032	0.0880	0.0501	0.0122
(0.50, 0.75)	150	0.9703	0.1638	1.1957	3.1611	0.6668	0.2371
	350	2.2291	0.1200	0.4611	3.3656	0.3557	0.2334
	550	3.4945	0.1376	0.1636	0.1967	0.4982	0.2717
(0.50, 0.50)	150	0.5338	0.0784	0.1924	0.1072	0.2682	0.2124
	350	0.8582	0.0434	0.0901	0.1528	0.2076	0.2134
	550	1.2480	0.0540	0.0396	0.1332	0.2796	0.2423
(0.50, 0.25)	150	0.6640	0.0522	0.0382	0.0994	0.2334	0.2191
	350	0.8259	0.0233	0.0207	0.1421	0.1564	0.2189
	550	1.0549	0.0304	0.0184	0.1772	0.1880	0.2499
(1, 0.75)	150	3.1793	0.5017	0.6227	3.3689	0.9971	0.7988
	350	7.3052	0.3878	0.3745	3.3869	0.7850	0.8163
	550	11.4313	0.3754	0.3416	0.5763	0.9343	0.8222
(1, 0.50)	150	1.7491	0.2599	0.3605	0.7276	0.4833	0.7203
	350	2.8124	0.1561	0.1923	0.8041	0.4716	0.7303
	550	4.0825	0.1743	0.1165	0.4573	0.5774	0.7667
(1, 0.25)	150	2.1756	0.1720	0.1144	0.7714	0.3197	0.7273
	350	2.7067	0.0774	0.0615	0.8935	0.3034	0.7255
	550	3.4510	0.1134	0.0572	0.5735	0.3942	0.7929

We observe that the [Horta & Ziegelmann's \(2018\)](#) method produces inferior accuracy because it ignores the density constraints. By obeying the density constraints, the remaining four methods improve the forecast accuracy. Among the four methods, the LQDT does not work well when functions have different finite supports, as evident from large $\overline{\text{KLD}}$ values. When the σ value is smaller, the nonparametric density-on-density regression using the functional Bayes NW estimator is the chosen method with the smallest $\overline{\text{KLD}}$. When the σ value is larger, and ρ_0 value is smaller, the CoDa method is preferred.

3.3 Analysis of a French COVID19 hospitalisation dataset

The French open data portal <https://www.data.gouv.fr/fr/> allows the general public to access many data sources. Simple research on this site with the keyword COVID19 leads us to several data sets. In this subsection, we are interested in the dynamics of the pandemic in France at the departmental level and, more particularly, in the hospitalisation data. French territory is divided into 101 administrative areas named départements. In Figure 6, we plot 96 departments located inside Europe.

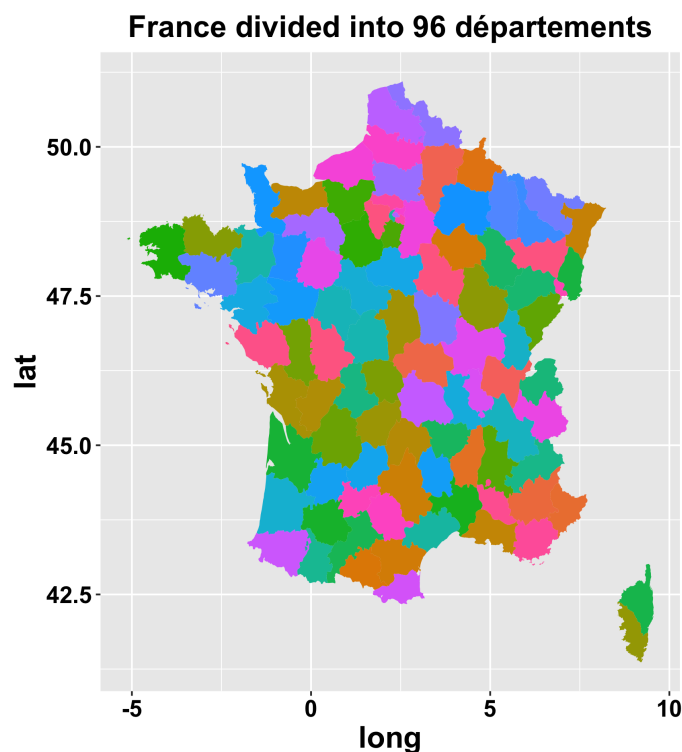


Figure 6 A map of French departments

The French COVID19 data, updated daily, are contained in a .csv file whose name starts with covid-hospit-2023 and can be downloaded <https://www.data.gouv.fr/fr/datasets/donnees>

[-hospitalieres-relatives-a-lepidemie-de-covid-19/](#). We are interested in studying the number of hospitalisations per 100,000 inhabitants for each department from March 18, 2020, to August 24, 2022. By focusing on cross-sectional data, we collect 96 daily hospitalisation ratios $(\mathcal{X}_{t,1}, \mathcal{X}_{t,2}, \dots, \mathcal{X}_{t,96})$ for each observed date $t = 1, 2, \dots, 890$. By taking a simple average over days, we can single out the departments with minimum and maximum hospitalisation ratios. The department Vendée has the minimum hospitalisation ratio, with an average of 8.58 per 100,000 inhabitants. The department Territoire de Belfort has the maximum hospitalisation ratio, with an average of 50.52 per 100,000 inhabitants.

Since the number of hospitalisation is nonnegative, it is an unnecessary constraint that can be removed via a natural logarithm transformation, denoted by $\ln(\cdot)$. Let $Z_{t,i} = \ln(\mathcal{X}_{t,i} + c)$ with $c > 0$ for $i = 1, 2, \dots, 96$, where c is an arbitrary small value such as $c = 0.1$. Then, we apply a kernel density estimator to estimate the probability density function f_t of Z_t without positive constraint. Computationally, the estimation is done via density function in [R](#) (R Core Team 2025) using Silverman's ROT bandwidth selection and truncated Gaussian kernel function. In Figure 7, we present the 890 estimated densities.

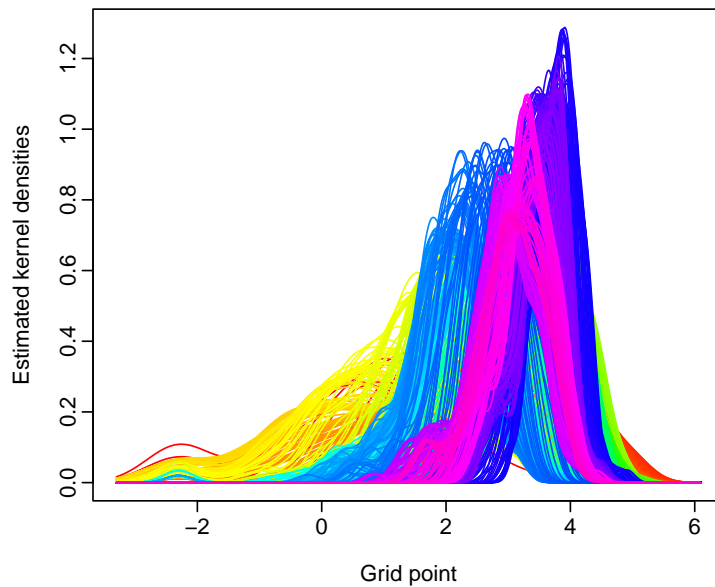


Figure 7 A time series of estimated probability density functions via a kernel density estimator with truncated Gaussian kernel and Silverman's ROT for the bandwidth selection. The estimated densities reflect daily COVID19 hospitalisation counts across the 96 departments.

From the estimated $(\hat{f}_1, \hat{f}_2, \dots, \hat{f}_{890})$, we split the samples into an initial training sample and a testing sample. The initial training sample consists of the first 594 estimated densities, while the testing sample consists of the remaining 296 estimated densities. Using the first 594 estimated

densities from March 18, 2020, to November 1, 2021, we produce one-step-ahead forecasts and evaluate its KLD with its holdout testing sample on November 2, 2021. Through an expanding window approach, we increase the training sample by one and use the first 595 estimated densities to produce one-step-ahead forecasts and evaluate its KLD on November 3, 2021. We proceed in the same manner to obtain 296 KLDs corresponding to the testing period.

In Figure 8, we present the 296 one-step-ahead density forecasts of the four methods considered. Since the regression mean function (i.e., signal) is unknown, the random walk is not considered a benchmark method. Compared with the holdout densities, we found the nonparametric density-on-density regression with the Bayes NW estimator performs the best. Similar to the CoDa method, it also uses the log-ratio transformation to remove constraints. A univariate functional time series forecasting method or a nonparametric function-on-function is then applied to obtain the forecasts. The forecasts are then back-transformed via the inverse log-ratio transformation. The nonparametric density-on-density regression with the Bayes NW estimator generally produces smoother density forecasts than the ones obtained from the CoDa method. The intuition is that the former one is a weighted average of the past densities and tends to be smooth.

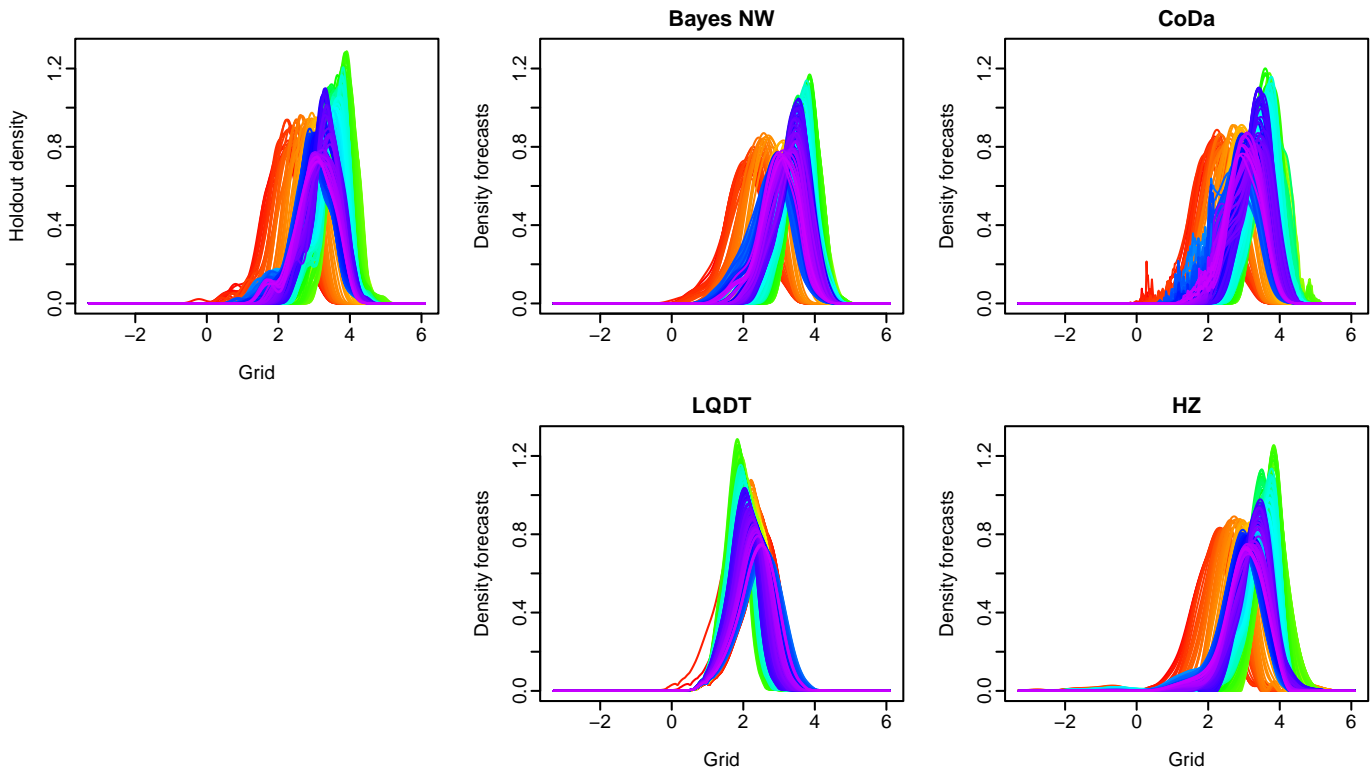


Figure 8 For the 296 holdout densities, we present the one-step-ahead density forecasts of the four methods based on an expanding window.

In Table 2, we present summary statistics of the KLDs obtained from the four methods. Based on the median and mean values, the nonparametric density-on-density regression with the Bayes NW estimator performs the best among the four methods.

Table 2 From the 296 KLDs, we present summary statistics for the four methods.

Statistic	Bayes NW	CoDa	LQDT	HZ
Min.	0.0041	0.0051	0.0171	0.0176
1st Qu.	0.0188	0.0197	1.0127	0.0727
Median	0.0293	0.0324	4.1861	0.1747
Mean	0.0420	0.0476	8.4794	0.2014
3rd Qu.	0.0524	0.0554	12.8809	0.2910
Max.	0.5241	0.4243	33.2268	0.9041

3.4 Analysis of age-specific life-table death counts in the United States

While it requires a way of estimating densities using a kernel estimator in Section 3.3, sometimes, we observe a time series of densities, such as period life table in demography and actuarial studies. A period life table is a table which shows, for each age, the probability that a person of that age will die before the next birthday. In the first age group, the initial number of alive is 100,000, while the remaining number of alive is 0 in the last age group. The sum of life-table death count is 100,000 every year, and the values are nonnegative, so these observations can be viewed as densities normalised to 100,000 rather than 1. By modelling the life-table death counts, we could understand a redistribution of survival probabilities, where deaths at younger ages gradually shift towards older ages. In Figure 1, we present rainbow plots of the female and male age distributions of life-table death counts in the USA from 1933 to 2023 in a single-year group.

Regarding the life-table death counts, we split the entire data set into a training sample from 1933 to 2000 and a testing sample from 2001 to 2023. Based on the initial training sample from 1933 to 2000, we compute the one-step-ahead density forecast in 2001 and the forecast error via the KLD. From the data in the training sample from 1933 to 2001, we again compute the one-step-ahead density forecast in 2002 and compute the forecast error. Then, we increase the training sample until the end of the testing samples. In Figure 9, we display the density forecasts computed by the nonparametric density-on-density regression with the Bayes NW estimator, CoDa method, LQDT method of Petersen & Müller (2016), and Horta & Ziegelmann’s (2018) method. Compared with the actual holdout samples, the Bayes NW estimator can adequately capture the local patterns,

especially for the male life-table death counts between ages 18 and 40.

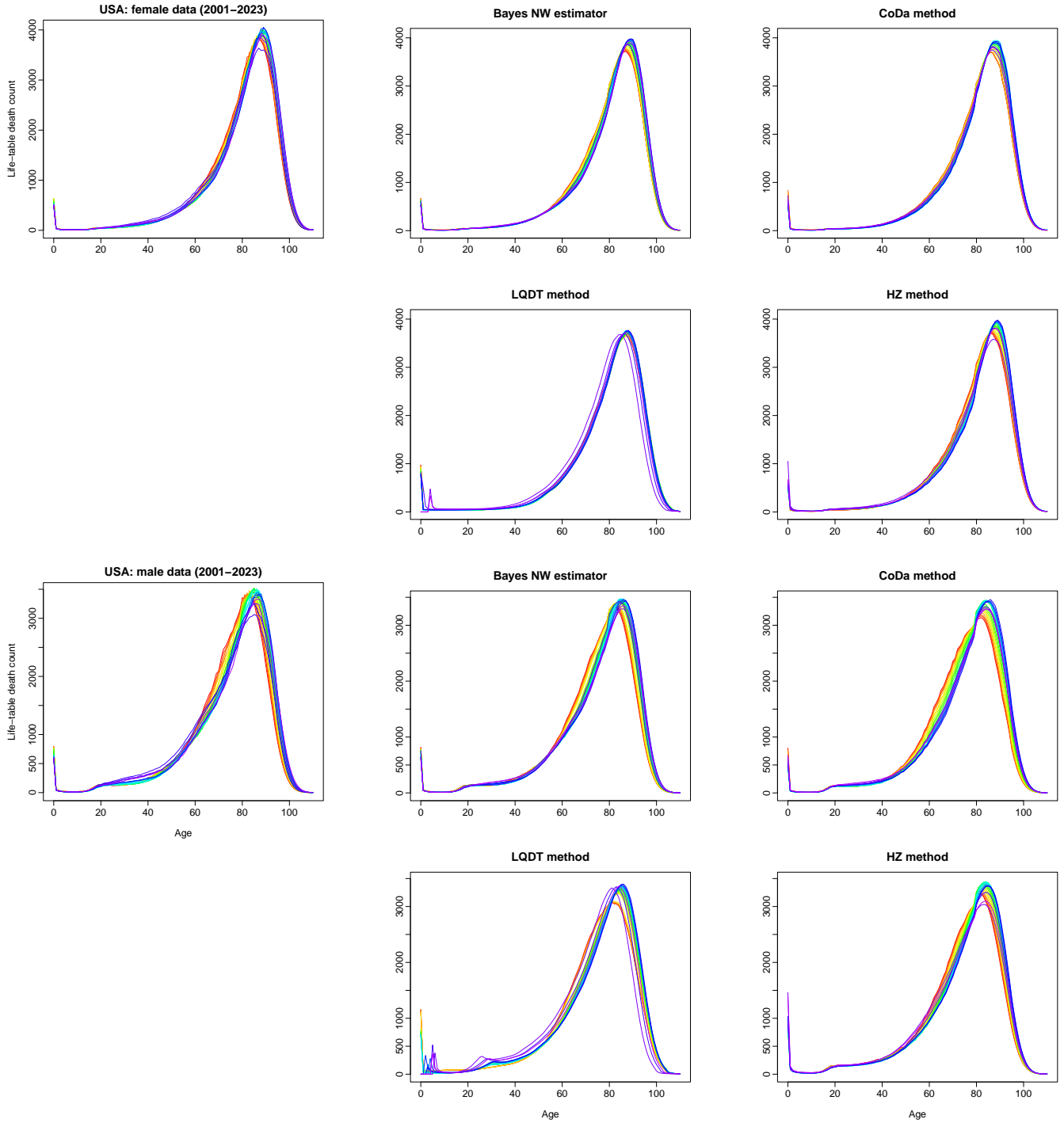


Figure 9 Holdout and forecast female and male life-table death counts from 2001 to 2023. The forecast life-table death counts were obtained via the nonparametric density-on-density regression with Bayes NW estimator, CoDa method, LQDT method, and HZ method, where the optimal bandwidth parameter was selected by the GCV.

With the optimal bandwidth parameter selected by the GCV, we iteratively compute the one-step-ahead density forecasts for years from 2001 to 2023, and then compute the overall KLDs in Figure 10.

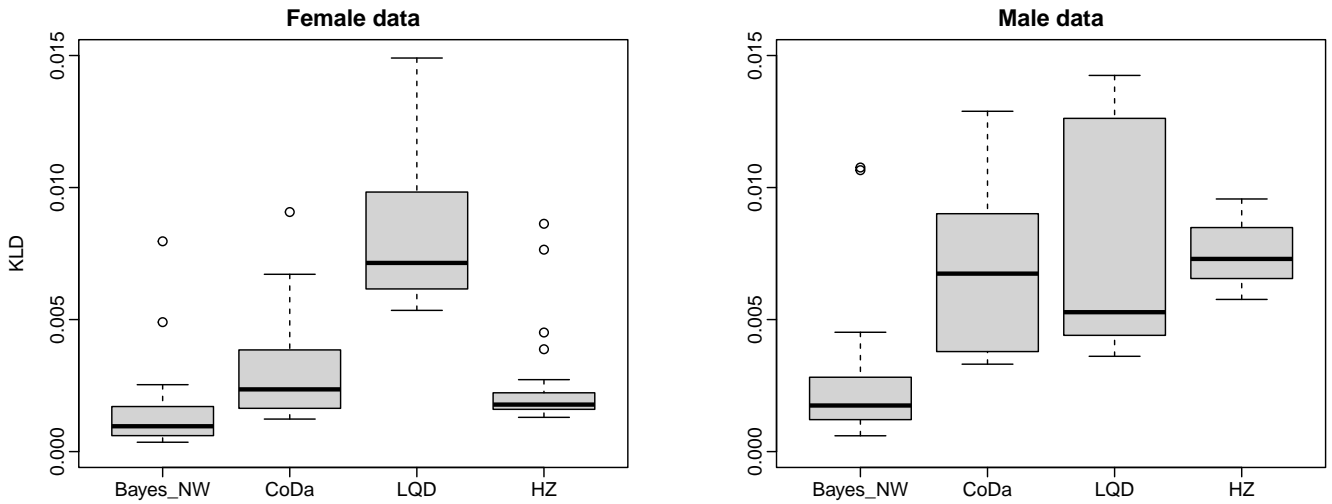



Figure 10 Forecast accuracy (MSPE ratios) between the nonparametric density-on-density regression using the Bayes NW, CoDa method, LQD method, and HZ method for forecasting one-step-ahead age-specific life-table death counts from 2001 to 2023 in the USA.

We evaluate and compare the KLD among the Bayes NW, CoDa, LQDT and HZ methods. The KLD of the nonparametric density-on-density regression with the Bayes NW estimator is the smallest among the four methods considered. The inferior performance of the LQDT method is primarily due to the left boundary problem, where there is a comparably higher number of deaths at the infant age.

4 Conclusion

We propose a nonparametric density-on-density regression with the Bayes NW estimator to model and forecast density-valued objects. The advantage of the nonparametric density-on-density regression is that the functional time series forecasts within the CoDa do not require a dimension reduction. In turn, there is no loss of information in the proposed method. Simulation and empirical data analyses demonstrate that the nonparametric density-on-density regression achieves good forecast accuracy.

Via a series of simulation studies, we show that the proposed method is competitive with several existing methods reported in [Kokoszka et al. \(2019\)](#). Since the true densities are often unobserved in empirical applications, we consider a kernel density estimator to estimate densities. The estimation accuracy of such an estimator depends on the kernel function type and bandwidth parameter selection. For estimating densities, we consider the truncated Gaussian kernel function,

and the optimal bandwidth is selected by either Silverman's ROT. For estimating the nonparametric estimator of the density-on-density regression, the optimal bandwidth parameter is selected by the GCV. With the selected bandwidth, we evaluate and compare the one-step-ahead forecast error between forecast densities constructed based on observed and estimated densities based on a kernel density estimator of the holdout observations using the expanding window approach. For reproducibility, the  code for the forecasting methods and their use in simulation and empirical data analyses are described in https://github.com/hanshang/Bayes_NW.

There are at least three ways the current paper can be further extended: First, a future extension is to develop a bandwidth procedure that jointly selects the optimal bandwidth parameters of the kernel density estimator and Bayes NW estimator. Second, comparing the predictive performance of different methods might not be as fruitful as one might think. It is hard to know when a predictive model works because everything is drowned in the incompressible randomness of new observations. The difference between competing methods can often be seen only in the digits of prediction error, even if they encode substantially different pictures of reality. One may achieve improved forecast accuracy by linearly combining the density forecasts from the nonparametric density-on-density regression and CoDa method. Finally, we proposed a Bayes NW estimator because of its simplicity. Its extension to Bayes local linear estimator can produce improved estimation accuracy.

Acknowledgments

The second author acknowledges financial support from an Australian Research Council Future Fellowship (grant no. FT240100338).

Appendices

A Preliminaries

Conditional expectation in $\mathcal{B}^2(I)$ and model. Let g and h two $\mathcal{B}^2(I)$ -valued random PDFs; for any f in $\mathcal{B}^2(I)$, the conditional expectation $E(g|h)$ is such that $\langle E(g|h), f \rangle_{\mathcal{B}} = E(\langle g, f \rangle_{\mathcal{B}}|h)$ (see, e.g., [Bosq 2000](#)). Then, $\langle E(f_{t+1}|f_t), g \rangle_{\mathcal{B}} = E(\langle f_{t+1}, g \rangle_{\mathcal{B}}|f_t)$ and (1) entails $\langle E(f_{t+1}|f_t), g \rangle_{\mathcal{B}} = E(\langle m(f_t) \oplus \epsilon_t, g \rangle_{\mathcal{B}}|f_t)$. With the property of the inner product, $\langle \cdot, \cdot \rangle_{\mathcal{B}}$, $\langle E(f_{t+1}|f_t), g \rangle_{\mathcal{B}} = E(\langle m(f_t), g \rangle_{\mathcal{B}}|f_t) + E(\langle \epsilon_t, g \rangle_{\mathcal{B}}|f_t) = \langle m(f_t), g \rangle_{\mathcal{B}} + \langle E(\epsilon_t|f_t), g \rangle_{\mathcal{B}}$. According to Model (1), $E(\epsilon_t|f_t) = \mathbf{0}_{\mathcal{B}}$ so that, for any g in $\mathcal{B}^2(I)$, $\langle E(f_{t+1}|f_t), g \rangle_{\mathcal{B}} = \langle m(f_t), g \rangle_{\mathcal{B}}$, which is equivalent to $m(f) = E(f_{t+1}|f_t = f)$.

Comparing $E(\|\hat{f}_t \ominus f_t\|_{\mathcal{B}}^2)$ and $MISE(\hat{f}_t)$. The next result gives a general situation where $\|f \ominus g\|_{\mathcal{B}}^2$ is smaller than $\|f - g\|$ up to a constant.

PROPOSITION 1 *Set $\theta > 0$; for any $f, g \in \mathcal{B}^2(I)$ with $f, g \geq \theta$, $\|f \ominus g\|_{\mathcal{B}}^2 = O(\|f - g\|^2)$.*

Proof. With the isometric feature of the clr transformation, $\|f \ominus g\|_{\mathcal{B}}^2 = \int_I \{\text{clr}(f) - \text{clr}(g)\}^2$, and the definition of clr results in $\|f \ominus g\|_{\mathcal{B}}^2 = \int_I (\log f - \log g)^2 + \frac{3}{b-a} \{\int_I (\log f - \log g)\}^2$. According to the Lipschitz property of the log function on $[\theta, +\infty[$, $|\log f(u) - \log g(u)| \leq \theta^{-1}|f(u) - g(u)|$ as soon as $f(u) \geq \theta$ and $g(u) \geq \theta$ for any u ; $\|f \ominus g\|_{\mathcal{B}}^2 \leq M_{\theta} \|f - g\|^2$ where $M_{\theta} = \theta^{-2}\{1 + 3/(b-a)\}$. As a by-product, if f is a density in $\mathcal{B}^2(I)$ such that $f \geq \theta > 0$, then $E(\|\hat{f}_t \ominus f_t\|_{\mathcal{B}}^2) = O\{MISE(\hat{f}_t)\}$.

B Proof of Theorem 1

Set $\hat{K}_t = K_r(h^{-1} \|\hat{f}_t \ominus f\|_{\mathcal{B}})$, $\hat{B} = (NE\hat{K}_1)^{-1} \sum_{t=1}^N \hat{K}_t$, $\hat{A} = (NE\hat{K}_1)^{-1} \odot \bigoplus_{t=1}^N (\hat{K}_t \odot \hat{f}_{t+1})$; the proof is based on the decomposition

$$\|\hat{m}_N(f) \ominus m(f)\|_{\mathcal{B}} \leq \hat{B}^{-1} \{Q_1 + Q_2\} + \hat{B}^{-1} \|m(f)\|_{\mathcal{B}} Q_3, \quad (4)$$

where $Q_1 = \|\hat{A} \ominus E\hat{A}\|_{\mathcal{B}}$, $Q_2 = \|E\hat{A} \ominus m(f)\|_{\mathcal{B}}$, and $Q_3 = |1 - \hat{B}|$. Before going on, let us point out useful features of the Bayes space $\mathcal{B}^2(I)$ properties that are systematically used in the proofs. First,

the Bayes space of bounded PDFs is a separable Hilbert space; it exists an orthonormal basis $\{e_j\}_{j \geq 1}$ such that, for any g in $\mathcal{B}^2(I)$, $g = \sum_{j \geq 1} \langle g, e_j \rangle_{\mathcal{B}}^2$. Second, the standard properties of norms naturally apply in $\mathcal{B}^2(I)$; for instance, for any u_1, u_2 in \mathbb{R} and any g_1, g_2 in $\mathcal{B}^2(I)$, $\|u_1 \odot g_1 \oplus u_2 \odot g_2\|_{\mathcal{B}} \leq |u_1| \|g_1\|_{\mathcal{B}} + |u_2| \|g_2\|_{\mathcal{B}}$. Third, with the assumptions on the kernel function (H6), it exists $C > 0$ and $C' > 0$ such that $C \pi_f(h_r) \leq \mathbb{E} K_1 \leq C' \pi_f(h_r)$ (resp. $C \hat{\pi}_f(h_r) \leq \mathbb{E} \hat{K}_1 \leq C' \hat{\pi}_f(h_r)$), where $\pi_f(h_r) = P(\|f_1 \ominus f\|_{\mathcal{B}} \leq h_r)$ (resp. $\hat{\pi}_f(h_r) = P(\|\hat{f}_1 \ominus f\|_{\mathcal{B}} \leq h_r)$). From now on, C and C' denote two generic strictly positive constants.

Focus on Q_1 . The separability property of the Bayes space $\mathcal{B}^2(I)$ entails the existence of an orthonormal basis $\{e_j\}_{j \geq 1}$ such that $\mathbb{E} Q_1^2 = \sum_{j \geq 1} \mathbb{E} \left(\langle \hat{A} \ominus \mathbb{E} \hat{A}, e_j \rangle_{\mathcal{B}}^2 \right)$. Let u_N be a sequence tending to infinity with N : $\mathbb{E} Q_1^2 = Q_{1,1} + Q_{1,2} + Q_{1,3}$ with $Q_{1,1} = (N \mathbb{E} \hat{K}_1)^{-2} \sum_{t=1}^N \sum_{j \geq 1} \text{Var} \left(\hat{K}_t \langle \hat{f}_{t+1}, e_j \rangle_{\mathcal{B}} \right)$, $Q_{1,2} = (N \mathbb{E} \hat{K}_1)^{-2} \sum_{s=1}^N \sum_{t=1}^N \sum_{j \geq 1} \text{cov}_{s,t,j}$, and $Q_{1,3} = (N \mathbb{E} \hat{K}_1)^{-2} \sum_{s=1}^N \sum_{t=1}^N \sum_{j \geq 1} \text{cov}_{s,t,j}$, where $\text{cov}_{s,t,j} = \text{Cov} \left(\hat{K}_s \langle \hat{f}_{s+1}, e_j \rangle_{\mathcal{B}}, \hat{K}_t \langle \hat{f}_{t+1}, e_j \rangle_{\mathcal{B}} \right)$. $Q_{1,1} \leq (N \mathbb{E} \hat{K}_1)^{-2} \sum_{t=1}^N \mathbb{E} \left(\hat{K}_t^2 \|\hat{f}_{t+1}\|_{\mathcal{B}}^2 \right)$ and $\|\hat{f}_{t+1}\|_{\mathcal{B}} \leq \|\hat{f}_{t+1} \ominus f_{t+1}\|_{\mathcal{B}} + \|f_{t+1} \ominus f\|_{\mathcal{B}} + \|f\|_{\mathcal{B}}$. (H3) and (H6) result in $\|\hat{f}_{t+1}\|_{\mathcal{B}} = O_P(1)$; $Q_{1,1} = O \left(\{N \hat{\pi}_f(h_r)\}^{-1} \right)$. With the Cauchy-Schwartz inequality and the dependence model, $\sum_{j \geq 1} |\text{cov}_{s,t,j}| \leq 2 \mathbb{E} \left(\hat{K}_1^2 \|\hat{f}_2\|_{\mathcal{B}}^2 \right)$; again, with (H3) and (H6), $Q_{1,2} = O \left(u_N \{N \hat{\pi}_f(h_r)\}^{-1} \right)$. According to the definition of ρ -mixing sequence, $\sum_{s=1}^N \sum_{t=1}^N \sum_{j \geq 1} |\text{cov}_{s,t,j}| \leq \rho(u_N) \mathbb{E} \left(\hat{K}_1^2 \|\hat{f}_2\|_{\mathcal{B}}^2 \right)$; then (H2) results in $Q_{1,3} = O \left(u_N^{-a} \hat{\pi}_f(h_r)^{-1} \right)$. If we set $u_N = N^{1/(a+1)}$, the quantity balancing $Q_{1,2}$ and $Q_{1,3}$, then $Q_1 = O_P \left(\left\{ N^{a/(a+1)} \hat{\pi}_f(h_r) \right\}^{-1/2} \right)$.

Focus on Q_2 . Taking into account the dependence model, $Q_2 = Q_{2,1} + Q_{2,2} + Q_{2,3}$ with $Q_{2,1} = (\mathbb{E} \hat{K}_1)^{-1} \mathbb{E} \left(\hat{K}_1 \|\hat{f}_2 \ominus f_2\|_{\mathcal{B}} \right)$, $Q_{2,2} = (\mathbb{E} \hat{K}_1)^{-1} \mathbb{E} \left(\hat{K}_1 \|m(f_1) \ominus m(f)\|_{\mathcal{B}} \right)$, $Q_{2,3} = (\mathbb{E} \hat{K}_1)^{-1} \left\| \mathbb{E} \left(\hat{K}_1 \odot \epsilon_1 \right) \right\|_{\mathcal{B}}$. Cauchy-Schwartz inequality with (H3) and (H6) entails $\mathbb{E} \left(\hat{K}_1 \|\hat{f}_2 \ominus f_2\|_{\mathcal{B}} \right) = O \left(\hat{\pi}_f(h_r)^{1/2} \delta_N \right)$; use again (H6) to get $Q_{2,1} = O \left(\hat{\pi}_f(h_r)^{-1/2} \delta_N \right)$. With the Lipschitz property of the regression operator m (see (H1)), $\|m(f_1) \ominus m(f)\|_{\mathcal{B}} \leq C \|f_1 \ominus f\|_{\mathcal{B}}$. Because we only retain f_t 's such that $K_t > 0$, $\|m(f_1) \ominus m(f)\|_{\mathcal{B}} \leq Ch$ and $Q_{2,2} = O(h_r)$. $\mathbb{E} (K_1 \odot \epsilon_1) = \mathbb{E} \{ \mathbb{E} (K_1 \odot \epsilon_1 | f_1) \}$: $\forall g \in \mathcal{B}^2(I)$, $\langle \mathbb{E} (K_1 \odot \epsilon_1 | f_1), g \rangle_{\mathcal{B}} = K_1 \langle \mathbb{E} (\epsilon_1 | f_1), g \rangle_{\mathcal{B}} = K_1 \langle \mathbf{0}_{\mathcal{B}}, g \rangle_{\mathcal{B}} = 0$. Conclusion: for any g in $\mathcal{B}^2(I)$, $\langle \mathbb{E} (K_1 \odot \epsilon_1 | f_1), g \rangle_{\mathcal{B}} = 0$, which results in $Q_{2,3} = 0$. All these intermediate results in $Q_2 = O(h_r) + O \left(\hat{\pi}_f(h_r)^{-1/2} \delta_N \right)$.

Remaining terms and summary. Q_3 is a particular case of Q_1 when $\hat{f}_{t+1} \equiv 1$ and $\hat{B} = 1 + (\hat{B} - 1)$

entails $\widehat{B} \leq 1 + Q_3$ so that $\widehat{B} = 1 + O_P \left(\left\{ N^{a/(a+1)} \widehat{\pi}_f(h_r) \right\}^{-1/2} \right)$. Then, the decomposition (4) results in

$$\|\widehat{m}_N(f) \ominus m(f)\|_{\mathcal{B}} = O(h_r) + O \left(\widehat{\pi}_f(h_r)^{-1/2} \delta_N \right) + O_P \left(\left\{ N^{a/(a+1)} \widehat{\pi}_f(h_r) \right\}^{-1/2} \right). \quad (5)$$

Comparison between $\widehat{\pi}_f(h_r)$ and $\pi_f(h_r)$. We now compare the asymptotic behaviour of $\pi_f(h)$ with those of $\widehat{\pi}_f(h)$. Indeed, according to (H3), it exists a sequence δ_N tending to 0 as N goes to infinity such that, $E \left(\|\widehat{f}_1 \ominus f_1\|_{\mathcal{B}}^2 \right) = O(\delta_N^2)$. Then, for any $C > 0$ and $b \in (1/3, 1)$, it exists $M > 0$, $P \left(\|\widehat{f}_1 \ominus f_1\|_{\mathcal{B}}^2 > C \delta_N^{1-b} \right) \leq M \delta_N^{2b}$. Set $\widehat{\mathcal{A}}_0 = \left\{ \|\widehat{f}_1 \ominus f_1\|_{\mathcal{B}} > C \delta_N^{1-b} \right\}$; $\widehat{\mathcal{A}} = \widehat{\mathcal{A}}_1 \cup \widehat{\mathcal{A}}_2$ with $\widehat{\mathcal{A}}_1 = \widehat{\mathcal{A}} \cap \widehat{\mathcal{A}}_0$ and $\widehat{\mathcal{A}}_2 = \widehat{\mathcal{A}} \cap \overline{\widehat{\mathcal{A}}_0}$ (see the previous focus on Q_2 for the definition of $\widehat{\mathcal{A}}$). Firstly, $P(\widehat{\mathcal{A}}_1) \leq P(\widehat{\mathcal{A}}_0) \leq M \delta_N^{2b}$, and secondly, $\|f \ominus f_1\|_{\mathcal{B}} < \|f \ominus \widehat{f}_1\|_{\mathcal{B}} + \|\widehat{f}_1 \ominus f_1\|_{\mathcal{B}}$ implies that $P(\widehat{\mathcal{A}}_2) \leq \pi_f(h + C \delta_N^{1-b})$. Because $P(\widehat{\mathcal{A}}) \leq P(\widehat{\mathcal{A}}_1) + P(\widehat{\mathcal{A}}_2)$, $P(\widehat{\mathcal{A}}) \leq \pi_f(h_r + C \delta_N^{1-b}) + M \delta_N^{2b}$; thanks to (H4) and (H5), it exists $C > 0$ such that $\widehat{\pi}_f(h_r) \leq C \pi_f(h_r)$. Now, set $\widehat{\mathcal{A}}_{\delta_N} = \left\{ \|\widehat{f}_1 \ominus f\|_{\mathcal{B}} < h_r - C \delta_N^{1-b} \right\}$, $\widehat{\mathcal{A}}_{\delta_N,1} = \widehat{\mathcal{A}}_{\delta_N} \cap \widehat{\mathcal{A}}_0$, and $\widehat{\mathcal{A}}_{\delta_N,2} = \widehat{\mathcal{A}}_{\delta_N} \cap \overline{\widehat{\mathcal{A}}_0}$. Because $P(\widehat{\mathcal{A}}_{\delta_N}) \leq P(\widehat{\mathcal{A}}_{\delta_N,1}) + P(\widehat{\mathcal{A}}_{\delta_N,2})$, $P(\widehat{\mathcal{A}}_{\delta_N}) \leq P(\widehat{\mathcal{A}}_0) + P(\widehat{\mathcal{A}})$, so that $\pi_f(h_r - C \delta_N^{1-b}) - M \delta_N^{2b} \leq P(\widehat{\mathcal{A}})$. Thanks to (H4) and (H5), it exists $C > 0$ such that $0 < C \pi_f(h_r) \leq \widehat{\pi}_f(h_r)$.

To end the proof of THEOREM 1, just replace $\widehat{\pi}_f(h_r)$ with $\pi_f(h_r)$ into (5).

References

- Aitchison, J. A. (1986), *The Statistical Analysis of Compositional Data*, Monographs on Statistics and Applied Probability, Chapman and Hall, London.
- Antoniadis, A., Paparoditis, E. & Sapatinas, T. (2006), 'A functional wavelet-kernel approach for time series prediction', *Journal of the Royal Statistical Society: Series B* **68**(5), 837–857.
- Antoniadis, A. & Sapatinas, T. (2003), 'Wavelet methods for continuous-time prediction using Hilbert-valued autoregressive processes', *Journal of Multivariate Analysis* **87**, 133–158.
- Bekierman, J. & Gribisch, B. (2021), 'A mixed frequency stochastic volatility model for intraday stock market returns', *Journal of Financial Econometrics* **19**(3), 496–530.
- Bergeron-Boucher, M.-P., Canudas-Romo, V., Oeppen, J. & Vaupel, J. W. (2017), 'Coherent forecasts of mortality with compositional data analysis', *Demographic Research* **37**, 527–566.
- Berlinet, A., Elamine, A. & Mas, A. (2011), 'Local linear regression for functional data', *Annals of the Institute of Statistical Mathematics* **63**(5), 1047–1075.
- Besse, P. C., Cardot, H. & Stephenson, D. B. (2000), 'Autoregressive forecasting of some functional climatic variations', *Scandinavian Journal of Statistics* **27**(4), 673–687.
- Biau, G. (2002), 'Optimal asymptotic quadratic errors of density estimators on random fields', *Statistics & Probability Letters* **60**(3), 297–307.
- Boj, E., Delicado, P. & Fortiana, J. (2010), 'Distance-based local linear regression for functional predictors', *Computational Statistics & Data Analysis* **54**(2), 429–437.
- Bosq, D. (2000), *Linear Processes in Function Spaces*, Vol. 149, Springer-Verlag, New York.
- Bradley, R. C. (2005), 'Basic properties of strong mixing conditions. a survey and some open questions', *Probability Surveys* **2**, 107–144.
- Burba, F., Ferraty, F. & Vieu, P. (2009), ' k -nearest neighbour method in functional nonparametric regression', *Journal of Nonparametric Statistics* **21**(4), 453–469.
- Castellana, J. V. & Leadbetter, M. R. (1986), 'On smoothed probability density estimation for stationary processes', *Stochastic Processes and Their Applications* **21**(2), 179–193.

- Chanda, K. C. (1983), 'Density estimation for linear processes', *Annals of the Institute of Statistical Mathematics* **35**(3), 439–446.
- Chesneau, C. (2014), 'A general result on the mean integrated squared error of the hard thresholding wavelet estimator under-mixing dependence', *Journal of Probability and Statistics* **2014**, Article ID 403764.
- Chiou, J.-M. & Müller, H.-G. (2009), 'Modeling hazard rates as functional data for the analysis of cohort lifetables and mortality forecasting', *Journal of the American Statistical Association: Applications and Case Studies* **104**(486), 572–585.
- Crainiceanu, C. M. & Goldsmith, A. J. (2010), 'Bayesian functional data analysis using WinBUGS', *Journal of Statistical Software* **32**(11), 1–33.
- Dai, X. (2022), 'Statistical inference on the Hilbert sphere with application to random densities', *Electronic Journal of Statistics* **16**, 700–736.
- Delicado, P. (2011), 'Dimensionality reduction when data are density functions', *Computational Statistics & Data Analysis* **55**(1), 401–420.
- Egozcue, J. J., Díaz-Barrero, J. L. & Pawlowsky-Glahn, V. (2006), 'Hilbert space of probability density functions based on Aitchison geometry', *Acta Mathematica Sinica* **22**(4), 1175–1182.
- Epanechnikov, V. A. (1969), 'Non-parametric estimation of a multivariate probability density', *Theory of Probability and its Applications* **14**, 153–158.
- Ferraty, F. & Nagy, S. (2022), 'Scalar-on-function local linear regression and beyond', *Biometrika* **109**(2), 439–455.
- Ferraty, F., Van Keilegom, I. & Vieu, P. (2012), 'Regression when both response and predictor are functions', *Journal of Multivariate Analysis* **109**, 10–28.
- Ferraty, F. & Vieu, P. (2006), *Nonparametric Functional Data Analysis*, Springer, New York.
- Ferraty, F., Zullo, A. & Fauvel, M. (2019), 'Nonparametric regression on contaminated functional predictor with application to hyperspectral data', *Econometrics and Statistics* **9**, 95–107.
- Hall, P. & Hart, J. (1990), 'Convergence rates in density estimation for data from infinite-order moving average processes', *Probability Theory and Related Fields* **87**(2), 253–274.

- Han, K., Müller, H.-G. & Park, B. U. (2020), 'Additive functional regression for densities as responses', *Journal of the American Statistical Association: Theory and Methods* **115**(530), 997–1010.
- Hansen, B. (2005), 'Exact mean integrated squared error of higher order kernel estimators', *Econometric Theory* **21**, 1031–1057.
- Hart, J. D. (1984), 'Efficiency of a kernel density estimator under an autoregressive dependence model', *Journal of the American Statistical Association: Theory and Methods* **79**(385), 110–117.
- Harvey, C. R., Liu, Y. & Zhu, H. (2016), '... and the cross-section of expected returns', *The Review of Financial Studies* **29**(1), 5–68.
- Hörmann, S. & Kokoszka, P. (2012), Functional time series, in T. S. Rao, S. S. Rao & C. R. Rao, eds, 'Handbook of Statistics', Vol. 30, North Holland, Amsterdam, pp. 157–186.
- Horta, E. & Ziegelmann, F. (2018), 'Dynamics of financial returns densities: A functional approach applied to the Bovespa intraday index', *International Journal of Forecasting* **34**(1), 75–88.
- Hron, K., Menafoglio, A., Templ, M., Hružová, K. & Filzmoser, P. (2016), 'Simplicial principal component analysis for density functions in Bayes spaces', *Computational Statistics & Data Analysis* **94**, 330–350.
- Hsing, T. & Eubank, R. (2015), *Theoretical Foundations of Functional Data Analysis, with an Introduction to Linear Operators*, Wiley Series in Probability and Statistics, New York.
- Human Mortality Database (2025), *University of California, Berkeley (USA), and Max Planck Institute for Demographic Research (Germany)*. Available at www.mortality.org or www.humanmortality.de (data downloaded on 25/March/2024).
- Hyndman, R. J. & Shang, H. L. (2009), 'Forecasting functional time series (with discussions)', *Journal of the Korean Statistical Society* **38**(3), 199–221.
- Jank, W., Shmueli, G., Plaisant, C. & Shneiderman, B. (2008), Visualizing functional data with an application to ebay's online auctions, in C.-H. Chen, W. Härdle & A. Unwin, eds, 'Handbook of Data Visualization', Springer, pp. 873–898.
- Joen, J. M. & Park, B. U. (2020), 'Additive regression with Hilbertian responses', *The Annals of Statistics* **48**(5), 2671–2697.

- Jones, M. C. & Rice, J. A. (1992), 'Displaying the important features of a large collection of similar curves', *The American Statistician* **46**(2), 140–145.
- Kneip, A. & Utikal, K. (2001), 'Inference for density families using functional principal component analysis', *Journal of the American Statistical Association: Theory and Methods* **96**(454), 519–532.
- Kokoszka, P., Miao, H., Petersen, A. & Shang, H. L. (2019), 'Forecasting of density functions with an application to cross-sectional and intraday returns', *International Journal of Forecasting* **35**(4), 1304–1317.
- Kokoszka, P. & Reimherr, M. (2017), *Introduction to Functional Data Analysis*, CRC Press, Boca Raton, Florida.
- Kokoszka, P., Rice, G. & Shang, H. L. (2017), 'Inference for the autocovariance of a functional time series under conditional heteroscedasticity', *Journal of Multivariate Analysis* **162**, 32–50.
- Kullback, S. & Leibler, R. A. (1951), 'On information and sufficiency', *The Annals of Mathematical Statistics* **22**(1), 79–86.
- Li, W. V. & Shao, Q.-M. (2001), Gaussian processes: inequalities, small ball probabilities and applications, in 'Handbook of Statistics', Vol. 19, Elsevier Science, p. 533–597.
- Lian, H. (2011), 'Convergence of functional k -nearest neighbor regression estimate with functional responses', *Electronic Journal of Statistics* **5**, 31–40.
- Lian, H. (2012), 'Convergence of nonparametric functional regression estimates with functional responses', *Electronic Journal of Statistics* **6**, 1373–1391.
- Marron, J. S. & Wand, M. P. (1992), 'Exact mean integrated squared error', *The Annals of Statistics* **20**(2), 712–736.
- Mateu, J. & Giraldo, R., eds (2022), *Geostatistical Functional Data Analysis*, Wiley series in probability and statistics, Wiley, Hoboken, New Jersey.
- Mazzuco, S. & Scarpa, B. (2015), 'Fitting age-specific fertility rates by a flexible generalized skew normal probability density function', *Journal of the Royal Statistical Society: Series A* **178**(1), 187–203.

- Menafooglio, A., Secchi, P. & Guadagnini, A. (2022), Geostatistical analysis in Bayes space: Probability densities and compositional data, in J. Mateu & R. Giraldo, eds, 'Geostatistical Functional Data Analysis', Wiley series in probability and statistics, Wiley, Hoboken, New Jersey, pp. 104–127.
- Nadaraya, E. A. (1974), 'On the integral mean square error of some nonparametric estimates for the density function', *Theory of Probability and its Applications* **19**, 133–141.
- Nerini, D. & Ghattas, B. (2007), 'Classifying densities using functional regression trees: Applications in oceanology', *Computational Statistics & Data Analysis* **51**(10), 4984–4993.
- Pawlowsky-Glahn, V., Egozcue, J. J. & Tolosana-Delgado, R. (2015), *Modeling and Analysis of Compositional Data*, John Wiley & Sons, Chichester, West Sussex.
- Petersen, A. & Müller, H.-G. (2016), 'Functional data analysis for density functions by transformation to a Hilbert space', *The Annals of Statistics* **44**, 183–218.
- Petersen, A. & Müller, H.-G. (2019), 'Wasserstein covariance for mutiple random densities', *Biometrika* **106**(2), 339–351.
- R Core Team (2025), *R: A Language and Environment for Statistical Computing*, R Foundation for Statistical Computing, Vienna, Austria.
 URL: <https://www.R-project.org/>
- Ramsay, J. O. & Silverman, B. W. (2005), *Functional Data Analysis*, 2nd edn, Springer, New York.
- Rio, E. (1993), 'Covariance inequalities for strongly mixing processes', *Ann. Inst. Henri. Poincaré Probabilités et Statistiques* **29**, 587–597.
- Robinson, P. M. (1986), 'On the consistency and finite-sample properties of nonparametric kernel time series regression, autoregression and density estimators', *Annals of the Institute of statistical Mathematics* **38**(3), 539–549.
- Rosenblatt, M. (1956), 'Remarks on some nonparametric estimates of a density function', *The Annals of Mathematical Statistics* **27**(3), 832–837.
- Rosenblatt, M. (1971), 'Curve estimates', *The Annals of Mathematical Statistics* **42**(6), 1815–1842.

- Rossi, F. & Villa, N. (2006), 'Support vector machine for functional data classification', *Neurocomputing* **69**(7-9), 730–742.
- Salazar, P., Napoli, D., Mario, J., Mostafa, J., Alibay, Z., Wendy, P., Alexander, M., Stephan, A., Bershad, E. M., Damani, R. & Divani, A. A. (2020), 'Exploration of multiparameter hematoma 3d image analysis for predicting outcome after intracerebral hemorrhage', *Neurocritical Care* **32**(2), 539–549.
- Seo, W.-K. & Beare, B. K. (2019), 'Cointegrated linear processes in Bayes Hilbert space', *Statistics & Probability Letters* **147**, 90–95.
- Shang, H. L. (2013), 'Bayesian bandwidth estimation for a nonparametric functional regression model with unknown error density', *Computational Statistics & Data Analysis* **67**, 185–198.
- Shang, H. L. (2017), 'Functional time series forecasting with dynamic updating: An application to intraday particulate matter concentration', *Econometrics and Statistics* **1**, 184–200.
- Shang, H. L., Cao, J. & Sang, P. (2022), 'Stopping time detection of wood panel compression: A functional time-series approach', *Journal of the Royal Statistical Society: Series C* **71**(5), 1205–1224.
- Shang, H. L. & Haberman, S. (2020), 'Forecasting age distribution of death counts: An application to annuity pricing', *Annals of Actuarial Science* **14**(1), 150–169.
- Shang, H. L. & Haberman, S. (2025a), 'Forecasting age distribution of deaths: Cumulative distribution function transformation', *Insurance: Mathematics and Economics* **in press**.
- Shang, H. L. & Haberman, S. (2025b), 'Forecasting age distribution of life-table death counts via α -transformation', *Scandinavian Actuarial Journal* **in press**.
- Srivastava, A., Klassen, E., Joshi, S. H. & Jermyn, I. H. (2011), 'Shape analysis of elastic curves in Euclidean spaces', *IEEE Transactions on Pattern Analysis and Machine Intelligence* **33**(7), 1415–1428.
- Van den Boogaart, K. G., Egozcue, J. J. & Pawlowsky-Glahn, V. (2010), 'Bayes linear spaces', *SORT: Statistics and Operations Research Transactions* **34**(4), 201–222.
- Van den Boogaart, K. G., Egozcue, J. J. & Pawlowsky-Glahn, V. (2014), 'Bayes Hilbert spaces', *Australian & New Zealand Journal of Statistics* **56**(2), 171–194.

- van der Linde, A. (2008), 'Variational Bayesian functional PCA', *Computational Statistics & Data Analysis* **53**(2), 517–533.
- Wang, J. (2012), A state space model approach to functional time series and time series driven by differential equations, PhD thesis, Rutgers University.
URL: <https://rucore.libraries.rutgers.edu/rutgers-lib/39059/pdf/1/>
- Wegman, E. J. (1972), 'Nonparametric probability density estimation: A comparison of density estimation methods', *Journal of Statistical Computation and Simulation* **1**, 225–245.
- Zhang, C., Kokoszka, P. & Petersen, A. (2022), 'Wasserstein autoregressive models for density time series', *Journal of Time Series Analysis* **43**(1), 30–52.